Review

A review of catalytic upgrading of bio-oil to engine fuels

P.M. Mortensen[a], J.-D. Grunwaldt[a,b], P.A. Jensen[a], K.G. Knudsen[c], A.D. Jensen[a,*]

[a] Department of Chemical and Biochemical Engineering, Technical University of Denmark, Søltofts Plads, Building 229, DK-2800 Lyngby, Denmark
[b] Institute of Chemical Technology and Polymer Science, Karlsruhe Institute of Technology (KIT), Engesserstrasse 20, D-79131 Karlsruhe, Denmark
[c] Haldor Topsø A/S, Nymøllevej 55, DK-2800 Lyngby, Denmark

ARTICLE INFO

ABSTRACT

As the oil reserves are depleting the need of an alternative fuel source is becoming increasingly apparent. One prospective method for producing fuels in the future is conversion of biomass into bio-oil and then upgrading the bio-oil over a catalyst, this method is the focus of this review article. Bio-oil production can be facilitated through flash pyrolysis, which has been identified as one of the most feasible routes. The bio-oil has a high oxygen content and therefore low stability over time and a low heating value. Upgrading is desirable to remove the oxygen and in this way make it resemble crude oil. Two general routes for bio-oil upgrading have been considered: hydrodeoxygenation (HDO) and zeolite cracking. HDO is a high pressure operation where hydrogen is used to exclude oxygen from the bio-oil, giving a high grade oil product equivalent to crude oil. Catalysts for the reaction are traditional hydrodesulphurization (HDS) catalysts, such as Co–MoS$_2$/Al$_2$O$_3$, or metal catalysts, as for example Pd/C. However, catalyst lifetimes of much more than 200 h have not been achieved with any current catalyst due to carbon deposition. Zeolite cracking is an alternative path, where zeolites, e.g. HZSM-5, are used as catalysts for the deoxygenation reaction. In these systems hydrogen is not a requirement, so operation is performed at atmospheric pressure. However, extensive carbon deposition results in very short catalyst lifetimes. Furthermore a general restriction in the hydrogen content of the bio-oil results in a low H/C ratio of the oil product as no additional hydrogen is supplied. Overall, oil from zeolite cracking is of a low grade, with heating values approximately 25% lower than that of crude oil. Of the two mentioned routes, HDO appears to have the best potential, as zeolite cracking cannot produce fuels of acceptable grade for the current infrastructure. HDO is evaluated as being a path to fuels in a grade and at a price equivalent to present fossil fuels, but several tasks still have to be addressed within this process. Catalyst development, understanding of the carbon forming mechanisms, understanding of the kinetics, elucidation of sulphur as a source of deactivation, evaluation of the requirement for high pressure, and sustainable sources for hydrogen are all areas which have to be elucidated before commercialisation of the process.

© 2011 Elsevier B.V. All rights reserved.

Contents

* Corresponding author. Tel.: +45 4525 2841; fax: +45 4588 2258.
  E-mail address: aj@kt.dtu.dk (A.D. Jensen).

1. Introduction

Energy consumption has never been higher worldwide than it is today, due to our way of living and the general fact that the World's population is increasing [1,2]. One of the main fields of energy consumption is the transportation sector, constituting about one fifth of the total [3]. As the World's population grows and means of transportation becomes more readily available, it is unavoidable that the need for fuels will become larger in the future [4]. This requirement constitutes one of the major challenges of the near future, as present fuels primarily are produced from crude oil and these reserves are depleting [5].

Substantial research is being carried out within the field of energy in order to find alternative fuels to replace gasoline and diesel. The optimal solution would be an alternative which is equivalent to the conventional fuels, i.e. compatible with the infrastructure as we know it, but also a fuel which is sustainable and will decrease the CO_2 emission and thereby decrease the environmental man-made footprint [6].

Biomass derived fuels could be the prospective fuel of tomorrow as these can be produced within a relatively short cycle and are considered benign for the environment [4,7]. So far first generation bio-fuels (bio-ethanol and biodiesel) have been implemented in different parts of the World [8,9]. However, these technologies rely on food grade biomass; first generation bio-ethanol is produced from the fermentation of sugar or starch and biodiesel is produced on the basis of fats [10–12]. This is a problem as the requirement for food around the World is a constraint and the energy efficiency per unit land of the required crops is relatively low (compared to energy crops) [13]. For this reason new research focuses on developing second generation bio-fuels, which can be produced from other biomass sources such as agricultural waste, wood, etc. Table 1 summarizes different paths for producing fuels from biomass and display which type of biomass source is required, showing that a series of paths exists which can utilise any source of biomass.

Of the second generation biofuel paths, a lot of efforts are presently spent on the biomass to liquid route via syngas to optimize the efficiency [14–17] and also synthesis of higher alcohols from syngas or hydrocarbons from methanol [16,18–22]. As an alternative, the estimated production prices shown in Table 1 indicate that HDO constitute a feasible route for the production of synthetic fuels. The competiveness of this route is achieved due to a good economy when using bio-oil as platform chemical (lower transport cost for large scale plants) and the flexibility with respect to the biomass feed [10,23–25]. Furthermore this route also constitute a path to fuels applicable in the current infrastructure [10].

Jointly, HDO and zeolite cracking are referred to as catalytic bio-oil upgrading and these could become routes for production of second generation bio-fuels in the future, but both routes are still far from industrial application. This review will give an overview on the present status of the two processes and also discuss which aspects need further elucidation. Each route will be considered independently. Aspects of operating conditions, choice of catalyst, reaction mechanisms, and deactivation mechanisms will be discussed. These considerations will be used to give an overview of the

Table 1
Overview of potential routes for production of renewable fuels from biomass. The prices are based on the lower heating value (LHV). Biomass as feed implies high flexibility with respect to feed source.

Technology	Feed	Platform chemical	Price [\$/toe[a]]
HDO	Biomass	Bio-oil	740[b]
Zeolite cracking	Biomass	Bio-oil	–
Fischer–Tropsch	Biomass	Syngas	840–1134[c]
H_2	Biomass	Syngas	378–714[d,e]
Methanol	Biomass	Syngas	546–588[f]
Higher alcohols	Biomass	Syngas	1302–1512[g]
Bio-ethanol	Sugar cane	–	369–922[h]
Bio-ethanol	Corn	–	1107–1475[i]
Bio-ethanol	Biomass	–	1475–2029[j]
Biodiesel	Canola oil	–	586–1171[k]
Biodiesel	Palm oil	–	586–937[l]
Gasoline	Crude oil	–	1046[m]

[a] toe: tonne of oil equivalent, 1 toe = 42 GJ.
[b] Published price: 2.04\$/gallon [167], 1 gallon = 3.7854 l, ρ = 719 kg/m^3, LHV = 42.5 MJ/kg.
[c] Published price: 20–27\$/GJ [197].
[d] Published price: 9–17\$/GJ [197,21].
[e] Expenses for distribution and storage are not considered.
[f] Published price: 13–14\$/GJ [197].
[g] Published price: 31–36\$/GJ [197].
[h] Published price: 0.2–0.5\$/l [193], ρ = 789 kg/m^3, LHV = 28.87 MJ/kg.
[i] Published price: 0.6–0.8\$/l [193].
[j] Published price: 0.8–1.1\$/l [193].
[k] Published price: 0.5–1\$/l [193], ρ = 832 kg/m^3, LHV = 43.1 MJ/kg.
[l] Published price: 0.5–0.8\$/l [193].
[m] Published price in USA April 2011: 2.88\$/gallon excluding distribution, marketing, and taxes [179]. Crude oil price April 2011: 113.23\$/barrel [196].

two processes compared to each other, but also relative to crude oil as the benchmark. Ultimately, an industrial perspective will be given, discussing the prospective of production of bio-fuels through catalytic bio-oil upgrading in industrial scale.

Other reviews within the same field are that by Elliott [26] from 2007 where the development within HDO since the 1980s is discussed, and a review in 2000 by Furimsky [27] where reaction mechanisms and kinetics of HDO are discussed. More general reviews of utilisation of bio-oil have been published by Zhang et al. [28], Bridgwater [29], and Czernik and Bridgwater [30], and reviews about bio-oil and production thereof have been published by Venderbosch and Prins [31] and Mohan et al. [32].

2. Bio-oil

As seen from Table 1, both HDO and zeolite cracking are based on bio-oil as platform chemical. Flash pyrolysis is the most widely applied process for production of bio-oil, as this has been found as a feasible route [16,26,33]. In this review, only this route will be discussed and bio-oil will in the following refer to flash pyrolysis oil. For information about other routes reference is made to [16,34–37].

Flash pyrolysis is a densification technique where both the mass- and energy-density is increased by treating the raw biomass at intermediate temperatures (300–600 °C) with high heating rates (10^3–10^4 K/s) and at short residence times (1–2 s) [28,31,38]. In this way, an increase in the energy density by roughly a factor of 7–8

Table 2
Bio-oil composition in wt% on the basis of different biomass sources and production methods.

	Corn cobs	Corn stover	Pine	Softwood	Hardwood
Ref. ♯	[45]	[45]	[50,31]	[195]	[195]
T [°C]	500	500	520	500	–
Reactor	Fluidized bed	Fluidized bed	Transport bed	Rotating bed	Transport bed
Water	25	9	24	29–32	20–21
Aldehydes	1	4	7	1–17	0–5
Acids	6	6	4	3–10	5–7
Carbohydrates	5	12	34	3–7	3–4
Phenolics	4	2	15	2–3	2–3
Furan etc.	2	1	3	0–2	0–1
Alcohols	0	0	2	0–1	0–4
Ketones	11	7	4	2–4	7–8
Unclassified	46	57	5	24–57	47–58

can be achieved [39,40]. Virtually any type of biomass is compatible with pyrolysis, ranging from more traditional sources such as corn and wood to waste products such as sewage sludge and chicken litter [38,41,42].

More than 300 different compounds have been identified in bio-oil, where the specific composition of the product depends on the feed and process conditions used [28]. In Table 2 a rough characterisation of bio-oil from different biomass sources is seen. The principle species of the product is water, constituting 10–30 wt%, but the oil also contains: hydroxyaldehydes, hydroxyketones, sugars, carboxylic acids, esters, furans, guaiacols, and phenolics, where many of the phenolics are present as oligomers [28,30,43,44].

Table 3 shows a comparison between bio-oil and crude oil. One crucial difference between the two is the elemental composition, as bio-oil contains 10–40 wt% oxygen [28,31,45]. This affects the homogeneity, polarity, heating value (HV), viscosity, and acidity of the oil.

The oxygenated molecules of lower molecular weight, especially alcohols and aldehydes, ensure the homogeneous appearance of the oil, as these act as a sort of surfactant for the higher molecular weight compounds, which normally are considered apolar and immiscible with water [166]. Overall this means that the bio-oil has a polar nature due to the high water content and is therefore immiscible with crude oil. The high water content and oxygen content further result in a low HV of the bio-oil, which is about half that of crude oil [28,31,30,46].

The pH of bio-oil is usually in the range from 2 to 4, which primarily is related to the content of acetic acid and formic acid [47]. The acidic nature of the oil constitutes a problem, as it will entail harsh conditions for equipment used for both storage, transport, and processing. Common construction materials such as carbon steel and aluminium have proven unsuitable when operating with bio-oil, due to corrosion [28,46].

A pronounced problem with bio-oil is the instability during storage, where viscosity, HV, and density all are affected. This is due to the presence of highly reactive organic compounds. Olefins are

suspected to be active for repolymerization in the presence of air. Furthermore, ketones, aldehydes, and organic acids can react to form ethers, acetales, and hemiacetals, respectively. These types of reactions effectively increase the average molecular mass of the oil, the viscosity, and the water content. An overall decrease in the oil quality is therefore seen as a function of storage time, ultimately resulting in phase separation [48–50].

Overall the unfavourable characteristics of the bio-oil are associated with the oxygenated compounds. Carboxylic acids, ketones, and aldehydes constitute some of the most unfavourable compounds, but utilisation of the oil requires a general decrease in the oxygen content in order to separate the organic product from the water, increase the HV, and increase the stability.

3. Bio-oil upgrading—general considerations

Catalytic upgrading of bio-oil is a complex reaction network due to the high diversity of compounds in the feed. Cracking, decarbonylation, decarboxylation, hydrocracking, hydrodeoxygenation, hydrogenation, and polymerization have been reported to take place for both zeolite cracking and HDO [51–53]. Examples of these reactions are given in Fig. 1. Besides these, carbon formation is also significant in both processes.

The high diversity in the bio-oil and the span of potential reactions make evaluation of bio-oil upgrading difficult and such evaluation often restricted to model compounds. To get a general thermodynamic overview of the process, we have evaluated the following reactions through thermodynamic calculations (based on data from Barin [54]):

$$phenol + H_2 \rightleftharpoons benzene + H_2O \qquad (1)$$

$$phenol + 4H_2 \rightleftharpoons cyclohexane + H_2O \qquad (2)$$
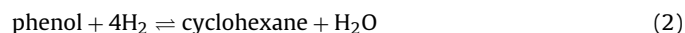
This reaction path of phenol has been proposed by both Massoth et al. [55] and Yunquan et al. [56]. Calculating the thermodynamic equilibrium for the two reactions shows that complete conversion of phenol can be achieved at temperatures up to at least 600 °C at atmospheric pressure and stoichiometric conditions. Increasing either the pressure or the excess of hydrogen will shift the thermodynamics even further towards complete conversion. Similar calculations have also been made with furfural, giving equivalent results. Thus, thermodynamics does not appear to constitute a constraint for the processes, when evaluating the simplest reactions of Fig. 1 for model compounds.

In practice it is difficult to evaluate the conversion of each individual component in the bio-oil. Instead two important parameters are the oil yield and the degree of deoxygenation:

$$Y_{oil} = \left(\frac{m_{oil}}{m_{feed}} \right) \cdot 100 \qquad (3)$$

Table 3
Comparison between bio-oil and crude oil. Data are from Refs. [10,11,28].

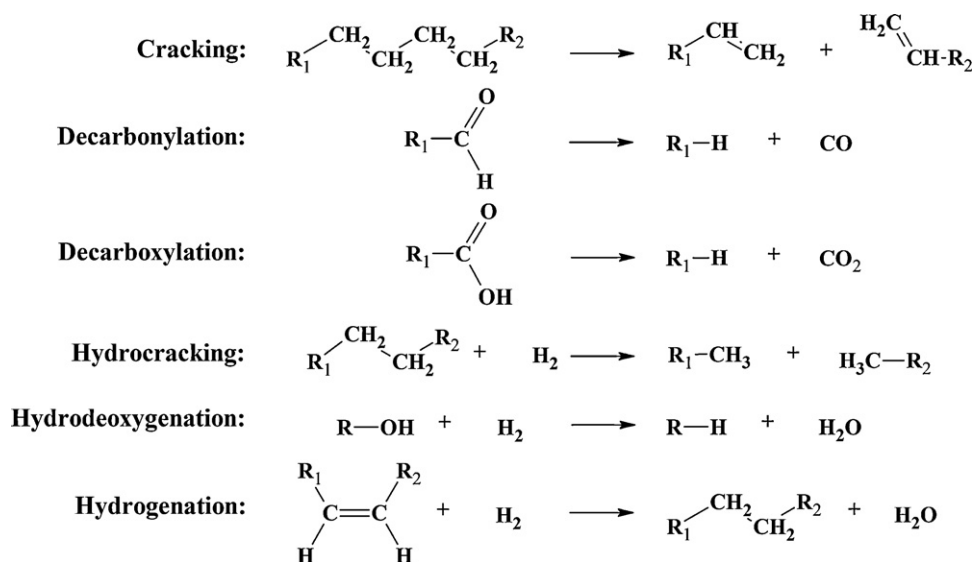|	Bio-oil	Crude oil
Water [wt%]	15–30	0.1
pH	2.8–3.8	–
ρ [kg/l]	1.05–1.25	0.86
$\mu_{50°C}$ [cP]	40–100	180
HHV [MJ/kg]	16–19	44
C [wt%]	55–65	83–86
O [wt%]	28–40	<1
H [wt%]	5–7	11–14
S [wt%]	<0.05	<4
N [wt%]	<0.4	<1
Ash [wt%]	<0.2	0.1

Fig. 1. Examples of reactions associated with catalytic bio-oil upgrading. The figure is drawn on the basis of information from Refs. [51,53].

$$DOD = \left(1 - \frac{wt\%_{O \text{ in product}}}{wt_{O \text{ in feed}}}\right) \cdot 100 \qquad (4)$$

Here Y_{oil} is the yield of oil, m_{oil} is the mass of produced oil, m_{feed} is the mass of the feed, DOD is the degree of deoxygenation, and $wt\%_O$ is the weight percent of oxygen in the oil. The two parameters together can give a rough overview of the extent of reaction, as the oil yield describes the selectivity toward an oil product and the degree of deoxygenation describes how effective the oxygen removal has been and therefore indicates the quality of the produced oil. However, separately the parameters are less descriptive, for it can be seen that a 100% yield can be achieved in the case of no reaction. Furthermore, none of the parameters relate to the removal of specific troublesome species and these would have to be analyzed for in detail.

Table 4 summarizes operating parameters, product yield, degree of deoxygenation, and product grade for some of the work conducted within the field of bio-oil upgrading. The reader can get an idea of how the choice of catalyst and operating conditions affect the process. It is seen that a wide variety of catalysts have been tested. HDO and zeolite cracking are split in separate sections in the table, where it can be concluded that the process conditions of HDO relative to zeolite cracking are significantly different, particularly with respect to operating pressure. The two processes will therefore be discussed separately in the following.

4. Hydrodeoxygenation

HDO is closely related to the hydrodesulphurization (HDS) process from the refinery industry, used in the elimination of sulphur from organic compounds [43,57]. Both HDO and HDS use hydrogen

Table 4
Overview of catalysts investigated for catalytic upgrading of bio-oil.

Catalyst	Setup	Feed	Time [h]	P [bar]	T [°C]	DOD [%]	O/C	H/C	Y_{oil} [wt%]	Ref. ♯
Hydrodeoxygenation										
Co–MoS$_2$/Al$_2$O$_3$	Batch	Bio-oil	4	200	350	81	0.8	1.3	26	[53]
Co–MoS$_2$/Al$_2$O$_3$	Continuous	Bio-oil	4[a]	300	370	100	0.0	1.8	33	[70]
Ni–MoS$_2$/Al$_2$O$_3$	Batch	Bio-oil	4	200	350	74	0.1	1.5	28	[53]
Ni–MoS$_2$/Al$_2$O$_3$	Continuous	Bio-oil	0.5[a]	85	400	28	–	–	84	[119]
Pd/C	Batch	Bio-oil	4	200	350	85	0.7	1.6	65	[53]
Pd/C	Continuous	Bio-oil	4[b]	140	340	64	0.1	1.5	48	[61]
Pd/ZrO$_2$	Batch	Guaiacol	3	80	300	–	0.1	1.3	–	[66]
Pt/Al$_2$O$_3$/SiO$_2$	Continuous	Bio-oil	0.5[a]	85	400	45	–	–	81	[119]
Pt/ZrO$_2$	Batch	Guaiacol	3	80	300	–	0.2	1.5	–	[66]
Rh/ZrO$_2$	Batch	Guaiacol	3	80	300	–	0.0	1.2	–	[66]
Ru/Al$_2$O$_3$	Batch	Bio-oil	4	200	350	78	0.4	1.2	36	[53]
Ru/C	Continuous	Bio-oil	0.2[a]	230	350–400	73	0.1	1.5	38	[11]
Ru/C	Batch	Bio-oil	4	200	350	86	0.8	1.5	53	[53]
Ru/TiO$_2$	Batch	Bio-oil	4	200	350	77	1.0	1.7	67	[53]
Zeolite cracking										
GaHZSM-5	Continuous	Bio-oil	0.32[a]	1	380	–	–	–	18	[130]
H-mordenite	Continuous	Bio-oil	0.56[a]	1	330	–	–	–	17	[145]
H–Y	Continuous	Bio-oil	0.28[a]	1	330	–	–	–	28	[145]
HZSM-5	Continuous	Bio-oil	0.32[a]	1	380	50	0.2	1.2	24	[130]
HZSM-5	Continuous	Bio-oil	0.91[a]	1	500	53	0.2	1.2	12	[127]
MgAPO-36	Continuous	Bio-oil	0.28[a]	1	370	–	–	–	16	[194]
SAPO-11	Continuous	Bio-oil	0.28[a]	1	370	–	–	–	20	[194]
SAPO-5	Continuous	Bio-oil	0.28[a]	1	370	–	–	–	22	[194]
ZnHZSM-5	Continuous	Bio-oil	0.32[a]	1	380	–	–	–	19	[130]

[a] Calculated as the inverse of the WHSV.
[b] Calculated as the inverse of the LHSV.

for the exclusion of the heteroatom, forming respectively H_2O and H_2S.

All the reactions shown in Fig. 1 are relevant for HDO, but the principal reaction is hydrodeoxygenation, as the name implies, and therefore the overall reaction can be generally written as (the reaction is inspired by Bridgwater [43,58] and combined with the elemental composition of bio-oil specified in Table 3 normalized to carbon):

$$CH_{1.4}O_{0.4} + 0.7 H_2 \rightarrow 1" CH_2" + 0.4 H_2O \qquad (5)$$
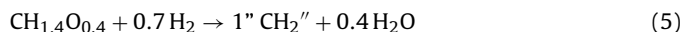
Here "CH_2" represent an unspecified hydrocarbon product. The overall thermo chemistry of this reaction is exothermic and simple calculations have shown an average overall heat of reaction in the order of 2.4 MJ/kg when using bio-oil [59].

Water is formed in the conceptual reaction, so (at least) two liquid phases will be observed as product: one organic and one aqueous. The appearance of two organic phases has also been reported, which is due to the production of organic compounds with densities less than water. In this case a light oil phase will separate on top of the water and a heavy one below. The formation of two organic phases is usually observed in instances with high degrees of deoxygenation, which will result in a high degree of fractionation in the feed [11].

In the case of complete deoxygenation the stoichiometry of Eq. (5) predicts a maximum oil yield of 56–58 wt% [43]. However, the complete deoxygenation indicated by Eq. (5) is rarely achieved due to the span of reactions taking place; instead a product with residual oxygen will often be formed. Venderbosch et al. [11] described the stoichiometry of a specific experiment normalized with respect to the feed carbon as (excluding the gas phase):

$$CH_{1.47}O_{0.56} + 0.39 H_2 \rightarrow 0.74 CH_{1.47}O_{0.11} + 0.19 CH_{3.02}O_{1.09}$$
$$+ 0.29 H_2O \qquad (6)$$
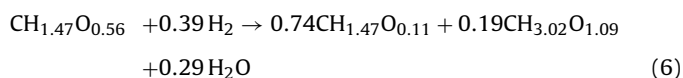
Here $CH_{1.47}O_{0.11}$ is the organic phase of the product and $CH_{3.02}O_{1.09}$ is the aqueous phase of the product. Some oxygen is incorporated in the hydrocarbons of the organic phase, but the O/C ratio is significantly lower in the hydrotreated organic phase (0.11) compared to the pyrolysis oil (0.56). In the aqueous phase a higher O/C ratio than in the parent oil is seen [11].

Regarding operating conditions, a high pressure is generally used, which has been reported in the range from 75 to 300 bar in the literature [31,60,61]. Patent literature describes operating pressures in the range of 10–120 bar [62,63]. The high pressure has been described as ensuring a higher solubility of hydrogen in the oil and thereby a higher availability of hydrogen in the vicinity of the catalyst. This increases the reaction rate and further decreases coking in the reactor [11,64]. Elliott et al. [61] used hydrogen in an excess of 35–420 mol H_2 per kg bio-oil, compared to a requirement of around 25 mol/kg for complete deoxygenation [11].

High degrees of deoxygenation are favoured by high residence times [31]. In a continuous flow reactor, Elliott et al. [61] showed that the oxygen content of the upgraded oil decreased from 21 wt% to 10 wt% when decreasing the LHSV from 0.70 h^{-1} to 0.25 h^{-1} over a Pd/C catalyst at 140 bar and 340 °C. In general LHSV should be in the order of 0.1–1.5 h^{-1} [63]. This residence time is in analogy to batch reactor tests, which usually are carried out over timeframes of 3–4 h [53,65,66].

HDO is normally carried out at temperatures between 250 and 450 °C [11,57]. As the reaction is exothermic and calculations of the equilibrium predicts potential full conversion of representative model compounds up to at least 600 °C, it appears that the choice of operating temperature should mainly be based on kinetic aspects. The effect of temperature was investigated by Elliott and Hart [61] for HDO of wood based bio-oil over a Pd/C catalyst in a fixed bed
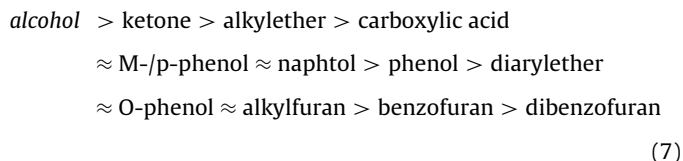
Table 5
Activation energy (E_A), iso-reactive temperature (T_{iso}), and hydrogen consumption for the deoxygenation of different functional groups or molecules over a Co–MoS$_2$/Al$_2$O$_3$ catalyst. Data are obtained from Grange et al. [23].

Molecule/group	E_A [kJ/mol]	T_{Iso} [°C]	Hydrogen consumption
Ketone	50	203	2 H_2/group
Carboxylic acid	109	283	3 H_2/group
Methoxy phenol	113	301	≈6 H_2/molecule
4-Methylphenol	141	340	≈4 H_2/molecule
2-Ethylphenol	150	367	≈4 H_2/molecule
Dibenzofuran	143	417	≈8 H_2/molecule

reactor at 140 bar. Here it was found that the oil yield decreased from 75% to 56% when increasing the temperature from 310 °C to 360 °C. This was accompanied by an increase in the gas yield by a factor of 3. The degree of deoxygenation increased from 65% at 310 °C to 70% at 340 °C. Above 340 °C the degree of deoxygenation did not increase further, but instead extensive cracking took place rather than deoxygenation.

The observations of Elliott et al. [61] are due to the reactivity of the different types of functional groups in the bio-oil [23,67]. Table 5 summarizes activation energies, iso-reactivity temperatures (the temperature required for a reaction to take place), and hydrogen consumption for different functional groups and molecules over a Co–MoS$_2$/Al$_2$O$_3$ catalyst. On this catalyst the activation energy for deoxygenation of ketones is relatively low, so these molecules can be deoxygenated at temperatures close to 200 °C. However, for the more complex bound or sterically hindered oxygen, as in furans or ortho substituted phenols, a significantly higher temperature is required for the reaction to proceed. On this basis the apparent reactivity of different compounds has been summarized as [27]:

$$alcohol > ketone > alkylether > carboxylic\ acid$$
$$\approx M\text{-}/p\text{-}phenol \approx naphtol > phenol > diarylether$$
$$\approx O\text{-}phenol \approx alkylfuran > benzofuran > dibenzofuran$$
$$(7)$$

An important aspect of the HDO reaction is the consumption of hydrogen. Venderbosch et al. [11] investigated hydrogen consumption for bio-oil upgrading as a function of deoxygenation rate over a Ru/C catalyst in a fixed bed reactor. The results are summarized in Fig. 2. The hydrogen consumption becomes increasingly steep as a function of the degree of deoxygenation.
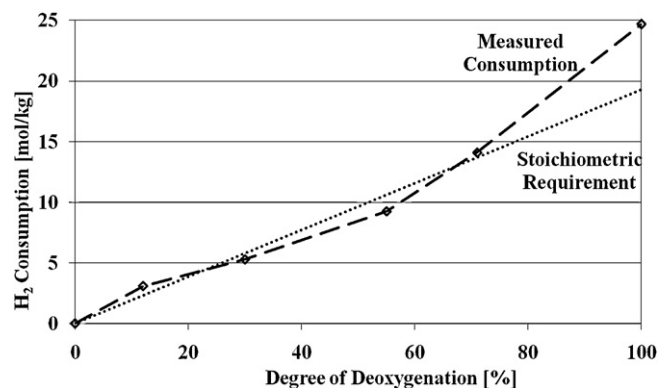

Fig. 2. Consumption of hydrogen for HDO as a function of degree of deoxygenation compared to the stoichiometric requirement. 100% deoxygenation has been extrapolated on the basis of the other points. The stoichiometric requirement has been calculated on the basis of an organic bound oxygen content of 31 wt% in the bio-oil and a hydrogen consumption of 1 mol H_2 per mol oxygen. Experiments were performed with a Ru/C catalyst at 175–400 °C and 200–250 bar in a fixed bed reactor fed with bio-oil. The high temperatures were used in order to achieve high degrees of deoxygenation. Data are from Venderbosch et al. [11].
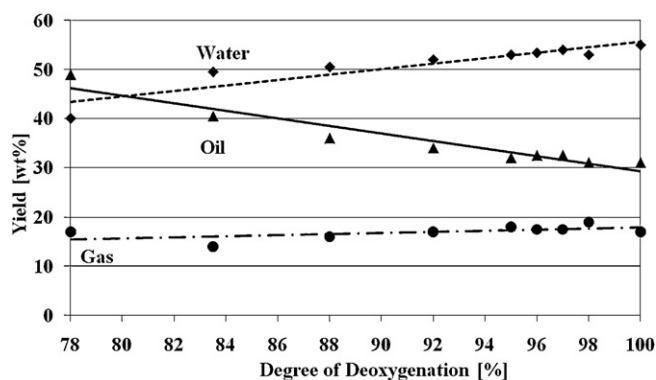
Fig. 3. Yields of oil, water, and gas from a HDO process as a function of the degree of deoxygenation. Experiments were performed with eucalyptus bio-oil over a Co–MoS$_2$/Al$_2$O$_3$ catalyst in a fixed bed reactor. Data are from Samolada et al. [81].

This development was presumed to be due to the different reactivity values of the compounds in the bio-oil. Highly reactive oxygenates, like ketones, are easily converted with low hydrogen consumption, but some oxygen is bound in the more stable compounds. Thus, the more complex molecules are accompanied by an initial hydrogenation/saturation of the molecule and therefore the hydrogen consumption exceeds the stoichiometric prediction at the high degrees of deoxygenation [27]. These tendencies are also illustrated in Table 5. Obviously, the hydrogen requirement for HDO of a ketone is significantly lower than that for a furan. Overall this means that in order to achieve 50% deoxygenation (ca. 25 wt% oxygen in the upgraded oil) 8 mol H$_2$ per kg bio-oil is required according to Fig. 2. In contrast, complete deoxygenation (and accompanied saturation) has a predicted hydrogen requirement of ca. 25 mol/kg, i.e. an increase by a factor of ca. 3.

The discussion above shows that the use of hydrogen for upgrading bio-oil has two effects with respect to the mechanism: removing oxygen and saturating double bounds. This results in decreased O/C ratios and increased H/C ratios, both of which increase the fuel grade of the oil by increasing the heating value (HV). Mercader et al. [60] found that the higher heating value (HHV) of the final product was approximately proportional to the hydrogen consumed in the process, with an increase in the HHV of 1 MJ/kg per mol/kg H$_2$ consumed.

In Fig. 3 the production of oil, water, and gas from a HDO process using a Co–MoS$_2$/Al$_2$O$_3$ catalyst is seen as a function of the degree of deoxygenation. The oil yield decreases as a function of the degree of deoxygenation, which is due to increased water and gas yields. This shows that when harsh conditions are used to remove the oxygen, a significant decrease in the oil yield occurs; it drops from 55% to 30% when increasing the degree of deoxygenation from 78% to 100%. It is therefore an important aspect to evaluate to which extent the oxygen should be removed [68].

4.1. Catalysts and reaction mechanisms

As seen from Table 4, a variety of different catalysts has been tested for the HDO process. In the following, these will be discussed as either sulphide/oxide type catalysts or transition metal catalysts, as it appears that the mechanisms for these two groups of catalysts are different.

4.1.1. Sulphide/oxide catalysts

Co–MoS$_2$ and Ni–MoS$_2$ have been some of the most frequently tested catalysts for the HDO reaction, as these are also used in the traditional hydrotreating process [26,27,64,67,69–83].

In these catalysts, Co or Ni serves as promoters, donating electrons to the molybdenum atoms. This weakens the bond between molybdenum and sulphur and thereby generates a sulphur vacancy site. These sites are the active sites in both HDS and HDO reactions [55,80,84–86].

Romero et al. [85] studied HDO of 2-ethylphenol on MoS$_2$-based catalysts and proposed the reaction mechanism depicted in Fig. 4. The oxygen of the molecule is believed to adsorb on a vacancy site of a MoS$_2$ slab edge, activating the compound. S–H species will also be present along the edge of the catalyst as these are generated from the H$_2$ in the feed. This enables proton donation from the sulphur to the attached molecule, which forms a carbocation. This can undergo direct C–O bond cleavage, forming the deoxygenated compound, and oxygen is hereafter removed in the formation of water.
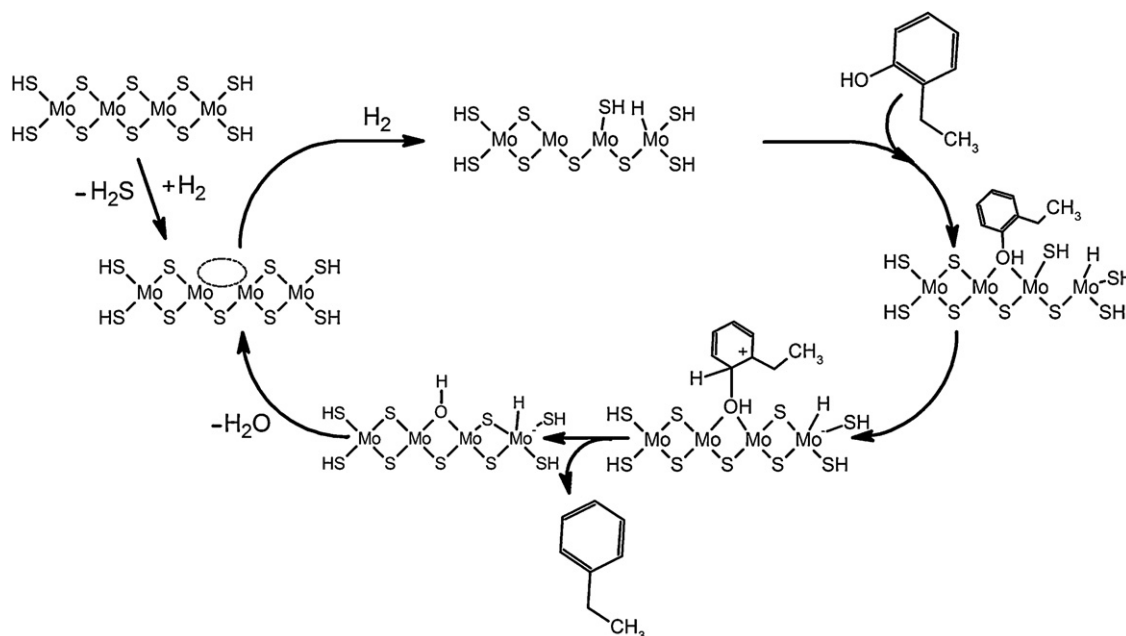

Fig. 4. Proposed mechanism of HDO of 2-ethylphenol over a Co–MoS$_2$ catalyst. The dotted circle indicates the catalytically active vacancy site. The figure is drawn on the basis of information from Romero et al. [85].

For the mechanism to work, it is a necessity that the oxygen group formed on the metal site from the deoxygenation step is eliminated as water. During prolonged operation it has been observed that a decrease in activity can occur due to transformation of the catalyst from a sulphide form toward an oxide form. In order to avoid this, it has been found that co-feeding H_2S to the system will regenerate the sulphide sites and stabilize the catalyst [79,84,87,88]. However, the study of Senol et al. [87,88] showed that trace amounts of thiols and sulphides was formed during the HDO of 3 wt% methyl heptanoate in m-xylene at 15 bar and 250 °C in a fixed bed reactor with Co–MoS_2/Al_2O_3 co-fed with up to 1000 ppm H_2S. Thus, these studies indicate that sulphur contamination of the otherwise sulphur free oil can occur when using sulphide type catalysts. An interesting perspective in this is that Co–MoS_2/Al_2O_3 is used as industrial HDS catalyst where it removes sulphur from oils down to a level of a few ppm [89]. On the other hand, Christensen et al. [19] showed that, when synthesizing higher alcohols from synthesisgas with Co–MoS_2/C co-fed with H_2S, thiols and sulfides were produced as well. Thus, the influence of the sulphur on this catalyst is difficult to evaluate and needs further attention.

On the basis of density functional theory (DFT) calculations, Moberg et al. [90] proposed MoO_3 as catalyst for HDO. These calculations showed that the deoxygenation on MoO_3 occur similar to the path in Fig. 4, i.e. chemisorption on a coordinatevely unsaturated metal site, proton donation, and desorption. For both oxide and sulphide type catalysts the activity relies on the presence of acid sites. The initial chemisorption step is a Lewis acid/base interaction, where the oxygen lone pair of the target molecule is attracted to the unsaturated metal site. For this reason it can be speculated that the reactivity of the system must partly rely on the availability and strength of the Lewis acid sites on the catalyst. Gervasini and Auroux [91] reported that the relative Lewis acid site surface concentration on different oxides are:

$$Cr_2O_3 > WO_3 > Nb_2O_5 > Ta_2O_5 > V_2O_5 \approx MoO_3 \qquad (8)$$
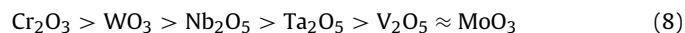
This should be matched against the relative Lewis acid site strength of the different oxides. This was investigated by Li and Dixon [92], where the relative strengths were found as:

$$WO_3 > MoO_3 > Cr_2O_3 \qquad (9)$$

The subsequent step of the mechanism is proton donation. This relies on hydrogen available on the catalyst, which for the oxides will be present as hydroxyl groups. To have proton donating capabilities, Brønsted acid hydroxylgroups must be present on the catalyst surface. In this context the work of Busca showed that the relative Brønsted hydroxyl acidity of different oxides is [90]:

$$WO_3 > MoO_3 > V_2O_5 > Nb_2O_5 \qquad (10)$$
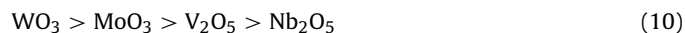
The trends of Eqs. (8)–(10) in comparison to the reaction path of deoxygenation reveals that MoO_3 functions as a catalyst due to the presence of both strong Lewis acid sites and strong Brønsted acid hydroxyl sites. However, Whiffen and Smith [93] investigated HDO of 4-methylphenol over unsupported MoO_3 and MoS_2 in a batch reactor at 41–48 bar and 325–375 °C, and found that the activity of MoO_3 was lower than that for MoS_2 and that the activation energy was higher on MoO_3 than on MoS_2 for this reaction. Thus, MoO_3 might not be the best choice of an oxide type catalyst, but on the basis of Eqs. (8)–(10) other oxides seem interesting for HDO. Specifically WO_3 is indicated to have a high availability of acid sites. Echeandia et al. [94] investigated oxides of W and Ni–W on active carbon for HDO of 1 wt% phenol in n-octane in a fixed bed reactor at 150–300 °C and 15 bar. These catalysts were all proven active for HDO and especially the Ni–W system had potential for complete conversion of the model compound. Furthermore, a low affinity for carbon was observed during the 6 h of experiments. This low
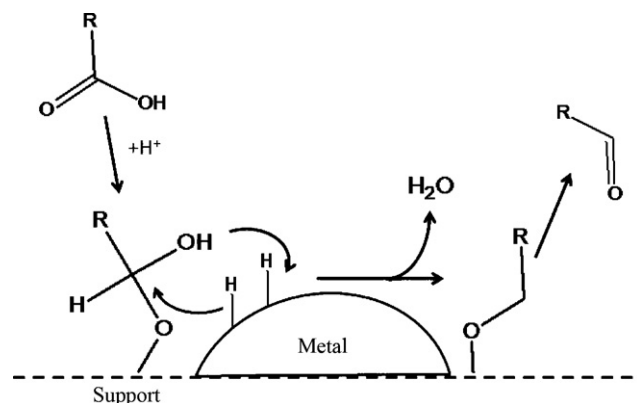

Fig. 5. HDO mechanism over transition metal catalysts. The mechanism drawn on the basis of information from Refs. [95,96].

value was ascribed to a beneficial effect from the non-acidic carbon support (cf. Section 4.1.3).

4.1.2. Transition metal catalysts

Selective catalytic hydrogenation can also be carried out with transition metal catalysts. Mechanistic speculations for these systems have indicated that the catalysts should be bifunctional, which can be achieved in other ways than the system discussed in Section 4.1.1. The bifunctionality of the catalyst implies two aspects. On one the hand, activation of oxy-compounds is needed, which likely could be achieved through the valence of an oxide form of a transition metal or on an exposed cation, often associated with the catalyst support. This should be combined with a possibility for hydrogen donation to the oxy-compound, which could take place on transition metals, as they have the potential to activate H_2 [95–98]. The combined mechanism is exemplified in Fig. 5, where the adsorption and activation of the oxy-compound are illustrated to take place on the support.

The mechanism of hydrogenation over supported noble metal systems is still debated. Generally it is acknowledged that the metals constitute the hydrogen donating sites, but oxy-compound activation has been proposed to either be facilitated on the metal sites [99–101] or at the metal-support interface (as illustrated in Fig. 5) [102,99,103]. This indicates that these catalytic systems potentially could have the affinity for two different reaction paths, since many of the noble metal catalysts are active for HDO.

A study by Gutierrez et al. [66] investigated the activity of Rh, Pd, and Pt supported on ZrO_2 for HDO of 3 wt% guaiacol in hexadecane in a batch reactor at 80 bar and 100 °C. They reported that the apparent activity of the three was:

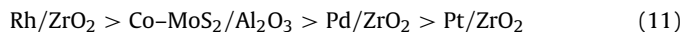$$Rh/ZrO_2 > Co-MoS_2/Al_2O_3 > Pd/ZrO_2 > Pt/ZrO_2 \qquad (11)$$

Fig. 6 shows the results from another study of noble metal catalysts by Wildschut et al. [53,104]. Here Ru/C, Pd/C, and Pt/C were investigated for HDO of beech bio-oil in a batch reactor at 350 °C and 200 bar over 4 h. Ru/C and Pd/C appeared to be good catalysts for the process as they displayed high degrees of deoxygenation and high oil yields, relative to Co–MoS_2/Al_2O_3 and Ni–MoS_2/Al_2O_3 as benchmarks.

Through experiments in a batch reactor setup with synthetic bio-oil (mixture of compounds representative of the real bio-oil) at 350 °C and ca. 10 bar of nitrogen, Fisk et al. [105] found that Pt/Al_2O_3 displayed catalytic activity for both HDO and steam reforming and therefore could produce H_2 in situ. This approach is attractive as the expense for hydrogen supply is considered as one of the disadvantages of the HDO technology. However, the catalyst was reported to suffer from significant deactivation due to carbon formation.
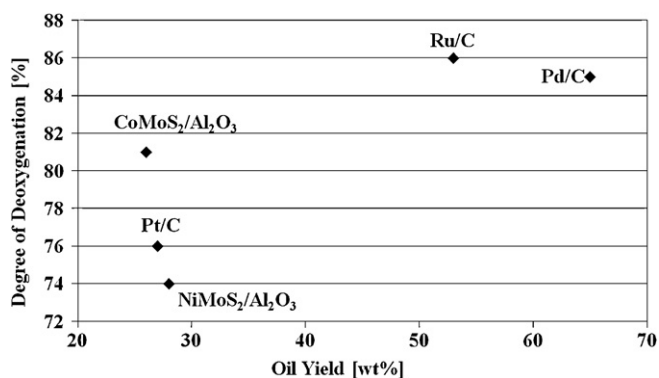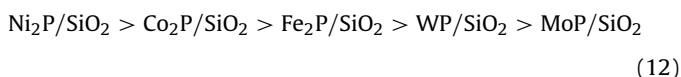
Fig. 6. Comparison of Ru/C, Pd/C, Pt/C, Co–MoS$_2$/Al$_2$O$_3$ and Ni–MoS$_2$/Al$_2$O$_3$ as catalysts for HDO, evaluated on the basis of the degree of deoxygenation and oil yield. Experiments were performed with beech bio-oil in a batch reactor at 350 °C and 200 bar over 4 h. Data are from Wildschut et al. [53,104].

To summarize, the noble metal catalysts Ru, Rh, Pd, and possibly also Pt appear to be potential catalysts for the HDO synthesis, but the high price of the metals make them unattractive.

As alternatives to the noble metal catalysts a series of investigations of base metal catalysts have been performed, as the prices of these metals are significantly lower [106]. Yakovlev et al. [98] investigated nickel based catalysts for HDO of anisole in a fixed bed reactor at temperatures in the range from 250 to 400 °C and pressures in the range from 5 to 20 bar. In Fig. 7 the results of these experiments are shown, where it can be seen that specifically Ni–Cu had the potential to completely eliminate the oxygen content in anisole. Unfortunately, this comparison only gives a vague idea about how the nickel based catalysts compare to other catalysts. Quantification of the activity and affinity for carbon formation of these catalysts relative to noble metal catalysts such as Ru/C and Pd/C or relative to Co–MoS$_2$ would be interesting.

Zhao et al. [107] measured the activity for HDO in a fixed bed reactor where a hydrogen/nitrogen gas was saturated with gaseous guaiacol (H$_2$/guaiacol molar ratio of 33) over phosphide catalysts supported on SiO$_2$ at atmospheric pressure and 300 °C. On this basis the following relative activity was found:

$$Ni_2P/SiO_2 > Co_2P/SiO_2 > Fe_2P/SiO_2 > WP/SiO_2 > MoP/SiO_2$$

(12)

All the catalysts were found less active than Pd/Al$_2$O$_3$, but more stable than Co–MoS$_2$/Al$_2$O$_3$. Thus, the attractiveness of these catalysts is in their higher availability and lower price, compared to noble metal catalysts.

A different approach for HDO with transition metal catalysts was published by Zhao et al. [108–110]. In these studies it was reported that phenols could be hydrogenated by using a heterogeneous aqueous system of a metal catalyst mixed with a mineral acid in a phenol/water (0.01 mol/4.4 mol) solution at 200–300 °C and 40 bar over a period of 2 h. In these systems hydrogen donation proceeds from the metal, followed by water extraction with the mineral acid, whereby deoxygenation can be achieved [109]. Both Pd/C and Raney® Ni (nickel-alumina alloy) were found to be effective catalysts when combined with Nafion/SiO$_2$ as mineral acid [110]. However, this concept has so far only been shown in batch experiments. Furthermore the influence of using a higher phenol concentration should be tested to evaluate the potential of the system.

Overall it is apparent that alternatives to both the sulphur containing type catalysts and noble metal type catalysts exist, but these systems still need additional development in order to evaluate their full potential.

4.1.3. Supports

The choice of carrier material is an important aspect of catalyst formulation for HDO [98].

Al$_2$O$_3$ has been shown to be an unsuitable support, as it in the presence of larger amounts of water it will convert to boemite (AlO(OH)) [11,26,111]. An investigation of Laurent and Delmon [111] on Ni–MoS$_2$/γ-Al$_2$O$_3$ showed that the formation of boemite resulted in the oxidation of nickel on the catalyst. These nickel oxides were inactive with respect to HDO and could further block other Mo or Ni sites on the catalyst. By treating the catalyst in a mixture of dodecane and water for 60 h, a decrease by two thirds of the activity was seen relative to a case where the catalyst had been treated in dodecane alone [26,111].

Additionally, Popov et al. [112] found that 2/3 of alumina was covered with phenolic species when saturating it at 400 °C in a phenol/argon flow. The observed surface species were believed to be potential carbon precursors, indicating that a high affinity for carbon formation exists on this type of support. The high surface coverage was linked to the relative high acidity of Al$_2$O$_3$.

As an alternative to Al$_2$O$_3$, carbon has been found to be a more promising support [53,94,113–115]. The neutral nature of carbon is advantageous, as this gives a lower tendency for carbon formation compared to Al$_2$O$_3$ [94,114]. Also SiO$_2$ has been indicated as a prospective support for HDO as it, like carbon, has a general neutral nature and therefore has a relatively low affinity for carbon formation [107]. Popov et al. [112] showed that the concentration of adsorbed phenol species on SiO$_2$ was only 12% relative to the concentration found on Al$_2$O$_3$ at 400 °C. SiO$_2$ only interacted with phenol through hydrogen bonds, but on Al$_2$O$_3$ dissociation of phenol to more strongly adsorbed surface species on the acid sites was observed [116].

ZrO$_2$ and CeO$_2$ have also been identified as potential carrier materials for the synthesis. ZrO$_2$ has some acidic character, but significantly less than Al$_2$O$_3$ [117]. ZrO$_2$ and CeO$_2$ are thought to have the potential to activate oxy-compounds on their surface, as shown in Fig. 5, and thereby increase activity. Thus, they seem attractive in the formulation of new catalysts, see also Fig. 7 [66,98,117,118].

Overall two aspects should be considered in the choice of support. On one hand the affinity for carbon formation should be low, which to some extent is correlated to the acidity (which should be low). Secondly, it should have the ability to activate oxy-compounds to facilitate sufficient activity. The latter is especially important when dealing with base metal catalysts, as discussed in Section 4.1.2.
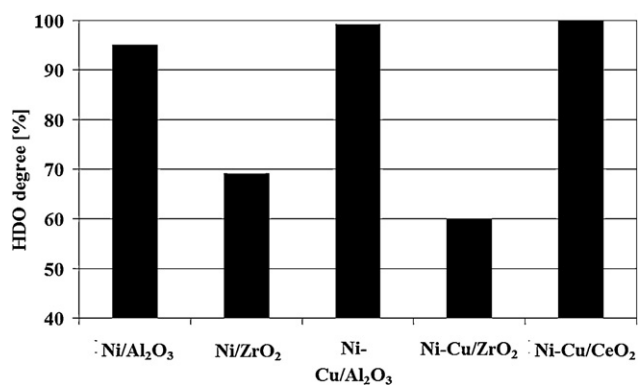

Fig. 7. Performance of nickel based catalysts for HDO. HDO degree is the ratio between the concentrations of oxygen free product relative to all products. Experiments performed with anisole in a fixed bed reactor at 300 °C and 10 bar. Data from Yakovlev et al. [98].

4.2. Kinetic models

A thorough review of several model compound kinetic studies has been made by Furimsky [27]. However, sparse information on the kinetics of HDO of bio-oil is available; here mainly lumped kinetic expressions have been developed, due to the diversity of the feed.

Sheu et al. [119] investigated the kinetics of HDO of pine bio-oil between ca. 300–400 °C over Pt/Al$_2$O$_3$/SiO$_2$, Co–MoS$_2$/Al$_2$O$_3$, and Ni–MoS$_2$/Al$_2$O$_3$ catalysts in a packed bed reactor. These were evaluated on the basis of a kinetic expression of the type:

$$-\frac{dw_{oxy}}{dZ} = k \cdot w_{oxy}^m \cdot P^n \tag{13}$$

Here w_{oxy} is the mass of oxygen in the product relative to the oxygen in the raw pyrolysis oil, Z is the axial position in the reactor, k is the rate constant given by an Arrhenius expression, P is the total pressure (mainly H$_2$), m is the reaction order for the oxygen, and n is the reaction order for the total pressure. In the study it was assumed that all three types of catalyst could be described by a first order dependency with respect to the oxygen in the pyrolysis oil (i.e. m = 1). On this basis the pressure dependency and activation energy could be found, which are summarized in Table 6. Generally a positive effect of an increased pressure was reported as n was in the range from 0.3 to 1. The activation energies were found in the range from 45.5 to 71.4 kJ/mol, with Pt/Al$_2$O$_3$/SiO$_2$ having the lowest activation energy. The lower activation energy for the Pt catalyst was in agreement with an observed higher degree of deoxygenation compared to the two other. The results of this study are interesting, however, the rate term of Eq. (13) has a non-fundamental form as the use of mass related concentrations and especially using the axial position in the reactor as time dependency makes the term very specific for the system used. Thus, correlating the results to other systems could be difficult. Furthermore, the assumption of a general first order dependency for w_{oxy} is a very rough assumption when developing a kinetic model.

A similar approach to that of Sheu et al. [119] was made by Su-Ping et al. [67], where Co–MoS$_2$/Al$_2$O$_3$ was investigated for HDO of bio-oil in a batch reactor between 360 and 390 °C. Here a general low dependency on the hydrogen partial pressure was found over a pressure interval from 15 bar to 30 bar, so it was chosen to omit the pressure dependency. This led to the expression:

$$-\frac{dC_{oxy}}{dt} = k \cdot C_{oxy}^{2.3} \tag{14}$$

Here C_{oxy} is the total concentration of all oxygenated molecules. A higher reaction order of 2.3 was found in this case, compared to the assumption of Sheu et al. [119]. The quite high apparent reaction order may be correlated with the activity of the different oxygen-containing species; the very reactive species will entail a high reaction rate, but as these disappear a rapid decrease in the rate will be observed (cf. discussion in Section 4). The activation energy was in this study found to be 91.4 kJ/mol, which is somewhat higher than that found by Sheu et al. [119].

Massoth et al. [55] on the other hand established a kinetic model of the HDO of phenol on Co–MoS$_2$/Al$_2$O$_3$ in a packed bed reactor based on a Langmuir–Hinshelwood type expression:

$$-\frac{dC_{Phe}}{d\tau} = \frac{k_1 \cdot K_{Ads} \cdot C_{Phe} + k_2 \cdot K_{Ads} \cdot C_{Phe}}{(1 + C_{Phe,0} \cdot K_{Ads} \cdot C_{Phe})^2} \tag{15}$$

Here C_{Phe} is the phenol concentration, $C_{Phe,0}$ the initial phenol concentration, K_{Ads} the equilibrium constant for adsorption of phenol on the catalyst, τ the residence time, and k_1 and k_2 rate constants for respectively a direct deoxygenation path (cf. Eq. (1)) and a hydrogenation path (cf. Eq. (2)). It is apparent that in order to describe HDO in detail all contributing reaction paths have to be regarded. This is possible when a single molecule is investigated. However, expanding this analysis to a bio-oil reactant will be too comprehensive, as all reaction paths will have to be considered.

Overall it can be concluded that describing the kinetics of HDO is complex due to the nature of a real bio-oil feed.

4.3. Deactivation

A pronounced problem in HDO is deactivation. This can occur through poisoning by nitrogen species or water, sintering of the catalyst, metal deposition (specifically alkali metals), or coking [59]. The extent of these phenomena is dependent on the catalyst, but carbon deposition has proven to be a general problem and the main path of catalyst deactivation [120].

Carbon is principally formed through polymerization and polycondensation reactions on the catalytic surface, forming polyaromatic species. This results in the blockage of the active sites on the catalysts [120]. Specifically for Co–MoS$_2$/Al$_2$O$_3$, it has been shown that carbon builds up quickly due to strong adsorption of polyaromatic species. These fill up the pore volume of the catalyst during the start up of the system. In a study of Fonseca et al. [121,122], it was reported that about one third of the total pore volume of a Co–MoS$_2$/Al$_2$O$_3$ catalyst was occupied with carbon during this initial carbon deposition stage and hereafter a steady state was observed where further carbon deposition was limited [120].

The rates of the carbon forming reactions are to a large extent controlled by the feed to the system, but process conditions also play an important role. With respect to hydrocarbon feeds, alkenes and aromatics have been reported as having the largest affinity for carbon formation, due to a significantly stronger interaction with the catalytic surface relative to saturated hydrocarbons. The stronger binding to the surface will entail that the conversion of the hydrocarbons to carbon is more likely. For oxygen containing hydrocarbons it has been identified that compounds with more than one oxygen atom appears to have a higher affinity for carbon formation by polymerization reactions on the catalysts surfaces [120].

Coking increases with increasing acidity of the catalyst; influenced by both Lewis and Brønsted acid sites. The principle function of Lewis acid sites is to bind species to the catalyst surface. Brønsted sites function by donating protons to the compounds of relevance, forming carbocations which are believed to be responsible for coking [120]. This constitute a problem as acid sites are also required in the mechanism of HDO (cf. Fig. 4). Furthermore, it has been found that the presence of organic acids (as acetic acid) in the feed will increase the affinity for carbon formation, as this catalyses the thermal degradation path [104].

In order to minimize carbon formation, measures can be taken in the choice of operating parameters. Hydrogen has been identified as efficiently decreasing the carbon formation on Co–MoS$_2$/Al$_2$O$_3$ as it will convert carbon precursors into stable molecules by saturating surface adsorbed species, as for example alkenes [120,123].

Table 6
Kinetic parameters for the kinetic model in Eq. (13) of different catalysts. Experiments performed in a packed bed reactor between ca. 300–400 °C and 45–105 bar. Data are from Sheu et al. [119].

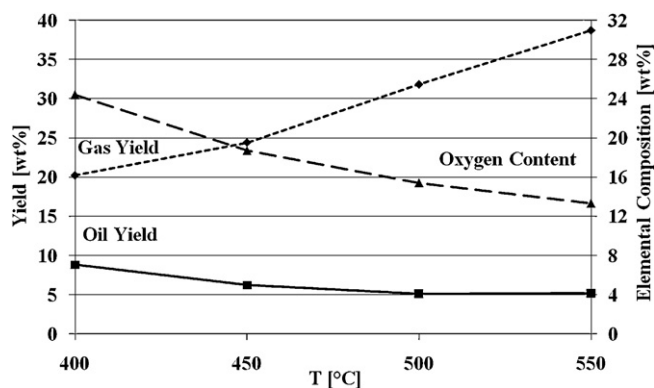| Catalyst	m	n	E_a [kJ/mol]]
Pt/Al$_2$O$_3$/SiO$_2$	1	1.0	45.5 ± 3.2
Co–MoS$_2$/Al$_2$O$_3$	1	0.3	71.4 ± 14.6
Ni–MoS$_2$/Al$_2$O$_3$	1	0.5	61.7 ± 7.1

Fig. 8. Yields of oil and gas compared to the elemental oxygen content in the oil from a zeolite cracking process as a function of temperature. Experiments were performed with a HZSM-5 catalyst in a fixed bed reactor for bio-oil treatment. Yields are given relative to the initial biomass feed. Data are from Williams and Horne [127].

Temperature also affects the formation of carbon. At elevated temperatures the rate of dehydrogenation increases, which gives an increase in the rate of polycondensation. Generally an increase in the reaction temperature will lead to increased carbon formation [120].

The loss of activity due to deposition of carbon on Co–MoS$_2$/Al$_2$O$_3$ has been correlated with the simple model [124]:

$$k = k_0 \cdot (1 - \Theta_C) \qquad (16)$$

Here k is the apparent rate constant, k_0 is the rate constant of an unpoisoned catalyst, and Θ_C is the fractional coverage of carbon on the catalyst's active sites. This expression describes the direct correlation between the extent of carbon blocking of the surface and the extent of catalyst deactivation and indicates an apparent proportional effect [120].

5. Zeolite cracking

Catalytic upgrading by zeolite cracking is related to fluid catalytic cracking (FCC), where zeolites are also used [57]. Compared to HDO, zeolite cracking is not as well developed at present, partly because the development of HDO to a large extent has been extrapolated from HDS. It is not possible to extrapolate zeolite cracking from FCC in the same degree [43,58,125].

In zeolite cracking, all the reactions of Fig. 1 take place in principle, but the cracking reactions are the primary ones. The conceptual complete deoxygenation reaction for the system can be characterized as (the reaction is inspired by Bridgwater [43,58] and combined with the elemental composition of bio-oil specified in Table 3 normalized to carbon):

$$CH_{1.4}O_{0.4} \rightarrow 0.9\text{``}CH_{1.2}\text{''} + 0.1\,CO_2 + 0.2\,H_2O \qquad (17)$$
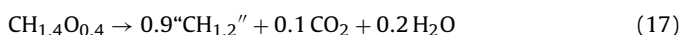
With "CH$_{1.2}$" being an unspecified hydrocarbon product. As for HDO, the bio-oil is converted into at least three phases in the process: oil, aqueous, and gas.

Typically, reaction temperatures in the range from 300 to 600 °C are used for the process [51,126]. Williams et al. [127] investigated the effect of temperature on HZSM-5 catalysts for upgrading of bio-oil in a fixed bed reactor in the temperature range from 400 to 550 °C, illustrated in Fig. 8. An increased temperature resulted in a decrease in the oil yield and an increase in the gas yield. This is due to an increased rate of cracking reactions at higher temperatures, resulting in the production of the smaller volatile compounds. However, in order to decrease the oxygen content to a significant degree the high temperatures were required. In conclusion, it is crucial to control the degree of cracking. A certain amount

of cracking is needed to remove oxygen, but if the rate of cracking becomes too high, at increased temperatures, degradation of the bio-oil to light gases and carbon will occur instead.

In contrast to the HDO process, zeolite cracking does not require co-feeding of hydrogen and can therefore be operated at atmospheric pressure. The process should be carried out with a relatively high residence time to ensure a satisfying degree of deoxygenation, i.e. LHSV around 2 h^{-1} [16]. However, Vitolo et al. [128] observed that by increasing the residence time, the extent of carbon formation also increased. Once again the best compromise between deoxygenation and limited carbon formation needs to be found.

In the case of complete deoxygenation the stoichiometry of Eq. (17) predicts a maximum oil yield of 42 wt%, which is roughly 15 wt% lower than the equivalent product predicted for HDO [43]. The reason for this lower yield is because the low H/C ratio of the bio-oil imposes a general restriction in the hydrocarbon yield [30]. The low H/C ratio of the bio-oil also affects the quality of the product, as the effective H/C ratio ((H/C)$_{eff}$) of the product from a FCC unit can be calculated as [57,129]:

$$(H/C)_{eff} = \frac{H - 2 \cdot O - 3 \cdot N - 2 \cdot S}{C} \qquad (18)$$

Here the elemental fractions are given in mol%. Calculating this ratio on the basis of a representative bio-oil (35 mol% C, 50 mol% H, and 15 mol% O, cf. Table 3) gives a ratio of 0.55. This value indicates that a high affinity for carbon exist in the process, as an H/C ratio toward 0 implies a carbonaceous product.

The calculated (H/C)$_{eff}$ values should be compared to the H/C ratio of 1.47 obtained for HDO oil in Eq. (6) and the H/C ratio of 1.5–2 for crude oil [10,11]. Some zeolite cracking studies have obtained H/C ratios of 1.2, but this has been accompanied with oxygen contents of 20 wt% [127,130].

The low H/C ratio of the zeolite cracking oil implies that hydrocarbon products from these reactions typically are aromatics and further have a generally low HV relative to crude oil [28,43].

Experimental zeolite cracking of bio-oil has shown yields of oil in the 14–23 wt% range [131]. This is significantly lower than the yields predicted from Eq. (17), this difference is due to pronounced carbon formation in the system during operation, constituting 26–39 wt% of the product [131].

5.1. Catalysts and reaction mechanisms

Zeolites are three-dimensional porous structures. Extensive work has been conducted in elucidating their structure and catalytic properties [132–137].

The mechanism for zeolite cracking is based on a series of reactions. Hydrocarbons are converted to smaller fragments through general cracking reactions. The actual oxygen elimination is associated with dehydration, decarboxylation, and decarbonylation, with dehydration being the main route [138].

The mechanism for zeolite dehydration of ethanol was investigated by Chiang and Bhan [139] and is illustrated in Fig. 9. The reaction is initiated by adsorption on an acid site. After adsorption, two different paths were evaluated, either a decomposition route or a bimolecular monomer dehydration (both routes are shown in Fig. 9). Oxygen elimination through decomposition was concluded to occur with a carbenium ion acting as a transition state. On this basis a surface ethoxide is formed, which can desorb to form ethylene and regenerate the acid site. For the bimolecular monomer dehydration, two ethanol molecules should be present on the catalyst, whereby diethylether can be formed. Preference for which of the two routes is favoured was concluded by Chiang and Bhan [139] to be controlled by the pore structure of the zeolite, with small pore structures favouring the less bulky ethylene product. Thus, product distribution is also seen to be controlled by the pore size, where
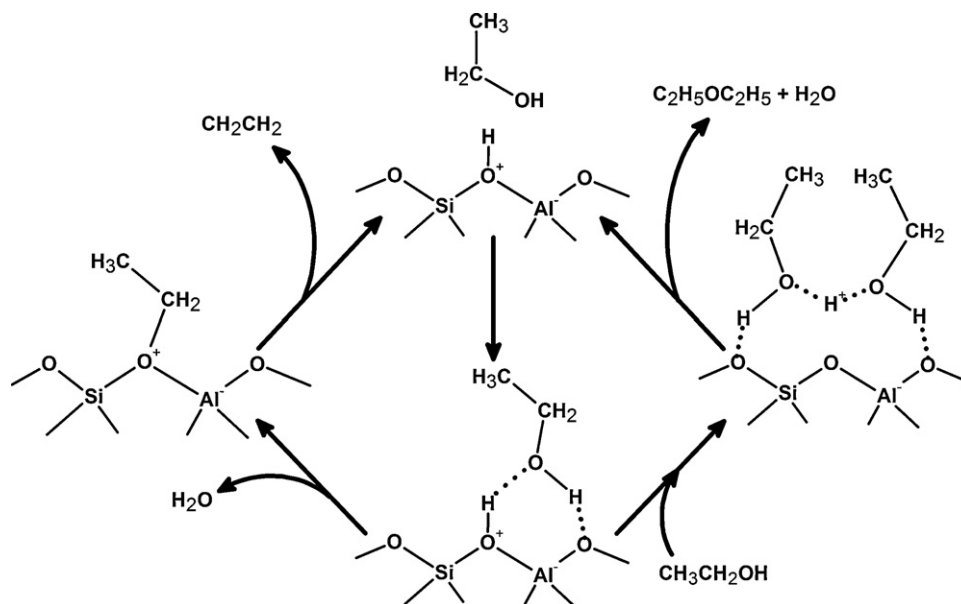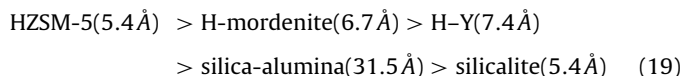
Fig. 9. Dehydration mechanism for ethanol over zeolites. The left route is the decomposition route and the right route is the bimolecular monomer dehydration. The mechanism is drawn on the basis of information from Chiand and Bhan [139].

deoxygenation of bio-oil in medium pore size zeolites (ca. 5–6 Å) gives increased production of C_6–C_9 compounds and larger pores (ca. 6–8 Å) gives increased production of C_9–C_12 [140].

The decomposition reactions occurring in the zeolite are accompanied by oligomerising reactions, which in the end produces a mixture of light aliphatic hydrocarbons (C_1–C_6) and larger aromatic hydrocarbons (C_6–C_10) [141]. The oligomerizing reaction mechanism is also based on the formation of carbenium ions as intermediates [142]. Thus, formation of carbenium ions is essential in all relevant reaction mechanisms [138,139,141–144].

In the choice of catalysts the availability of acid sites is important. This tendency has also been described for petroleum cracking zeolites, where a high availability of acid sites leads to extensive hydrogen transfer and thereby produces a high gasoline fraction. However, carbon forming mechanisms are also driven by the hydrogen transfer, so the presence of many acid sites will also increase this fraction. When discussing aluminosilicate zeolites the availability of acid sites is related to the Si/Al ratio, where a high ratio entails few alumina atoms in the structure leading to few acid sites, and a low Si/Al ratio entails many alumina atoms in the structure, leading to many acid sites [143].

Different types of zeolites have been investigated for the zeolite cracking process of both bio-oil and model compounds, as seen from Table 4, with HZSM-5 being the most frequently tested [51,128,130,140,141,144–152,159,154]. Adjaye et al. [140,145] performed some of the initial catalyst screening studies by investigating HZSM-5, H-mordenite, H-Y, silica-alumina, and silicalite in a fixed bed reactor fed with aspen bio-oil and operated between 330 and 410 °C. In these studies it was found that the activity of the catalysts followed the order:

$$HZSM\text{-}5(5.4\text{Å}) > H\text{-mordenite}(6.7\text{Å}) > H\text{-Y}(7.4\text{Å})$$
$$> \text{silica-alumina}(31.5\text{Å}) > \text{silicalite}(5.4\text{Å}) \quad (19)$$

With the number in the parentheses being the average pore sizes of the zeolites. Practically, silicalite does not contain any acid sites as it is a polymorph structure of Si. In comparison, HZSM-5 is rich in both Lewis and Brønsted acid sites. The above correlation therefore shows that the activity of zeolite cracking catalysts are highly dependent on the availability of acid sites [140].

Overall, tuning of the acid sites availability is important in designing the catalyst, as it affects the selectivity of the system, but also the extent of carbon formation. Many acid sites give a high yield of gasoline, but this will also lead to a high affinity for carbon formation as both reactions are influenced by the extent of acid sites [143].

5.2. Kinetic models

Only a few kinetic investigations have been reported for zeolite cracking systems. On the basis of a series of model compound studies, Adjaye and Bakshi [51,126] found that the reaction network in zeolite cracking could be described as sketched in Fig. 10. They suggested that the bio-oil initially separates in two fractions, a volatile and a non-volatile fraction (differentiated by which molecules evaporated at 200 °C under vacuum). The non-volatile fraction can be converted into volatiles due to cracking reactions. Besides this, the non-volatiles can either polymerize to form residue or condensate/polymerize to form carbon, with residue being the fraction of the produced oil which does not evaporate during vacuum distillation at 200 °C. The volatile fraction is associated with the formation of the three fractions in the final product: the oil fraction, the aqueous fraction, and the gas fraction. Furthermore the volatiles can react through polymerization or condensation reactions to form residue or carbon.
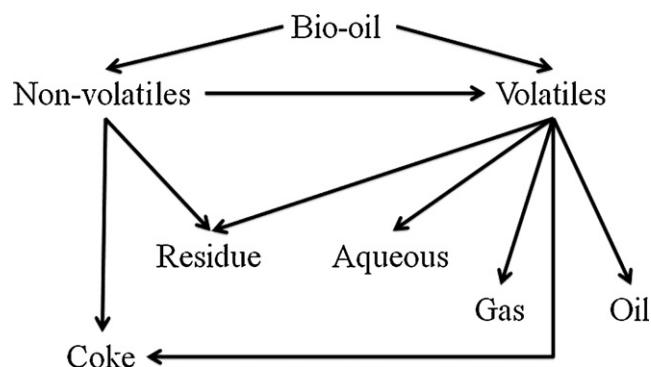

Fig. 10. Reaction network for the kinetic model described in Eqs. (20)–(26).

This reaction network was used in the formulation of a kinetic model, which was fitted to experiments with aspen bio-oil over HZSM-5 in the temperature range from 330 to 410 °C:

Nonvolatiles : $\dfrac{dC_{NV}}{dt} = k_{NV} \cdot C_B - k_{Cr} \cdot C_{NV}^{0.9} - k_{R1} \cdot C_{NV}^{r1} - k_{C1} \cdot C_{NV}^{c1}$

$$(20)$$

Volatiles : $\dfrac{dC_V}{dt} = k_V \cdot C_B + k_{Cr} \cdot C_{NV}^{0.9} - k_{Oil} \cdot C_V^{o} - k_{Gas} \cdot C_V^{g}$

$$- k_{Aqua} \cdot C_V^{a} - k_{R2} \cdot C_V^{r2} - k_{C2} \cdot C_V^{c2} \qquad (21)$$

Oil : $\dfrac{dC_{Oil}}{dt} = k_{Oil} \cdot C_V^{o}$ $\qquad (22)$

Aqueous : $\dfrac{dC_{Aqua}}{dt} = k_{Aqua} \cdot C_V^{a}$ $\qquad (23)$

Gas : $\dfrac{dC_{Gas}}{dt} = k_{Gas} \cdot C_V^{g}$ $\qquad (24)$

Carbon : $\dfrac{dC_C}{dt} = k_{C1} \cdot C_{NV}^{c1} + k_{C2} \cdot C_V^{c2}$ $\qquad (25)$

Residue : $\dfrac{dC_R}{dt} = k_{R1} \cdot C_{NV}^{r1} + k_{R2} \cdot C_V^{r2}$ $\qquad (26)$

Here C_i is the concentration of i, k_i is the rate constant of reaction i, index B means bio-oil, index Cr means cracking, o is the reaction order for oil formation (decreasing from 1 to 0.8 with increasing T), a is the reaction order for the aqueous phase formation (in the interval from 1.4 to 1.6), g is the reaction order for gas formation (increasing from 0.7 to 0.8 with increasing T), $c1$ is the reaction order for carbon formation from non-volatiles (increasing from 0.9 to 1.1 with T), $c2$ is the reaction order for carbon formation from volatiles (ranging from 1.1 to 1.2 with increasing T), $r1$ is the reaction order for carbon formation from non-volatiles (increasing from 1.9 to 2.5 with increasing T), and $r2$ is the reaction order for carbon formation from volatiles (decreasing from 1.5 to 0.7 with increasing T).

Fig. 11 shows a fit between the model and representative data. Overall the model succeeded in reproducing the experimental data adequately, but this was done on the basis of variable reaction orders, as mentioned above. Thus, the model becomes insufficient to describe the rate correlation in any broad context.

Overall the results of Adjaye and Bakshi [51,126] display the same problems as observed in the kinetic systems discussed for HDO (Section 4.2); the complexity of the feed makes it difficult to create a kinetic description of the system without making a compromise.
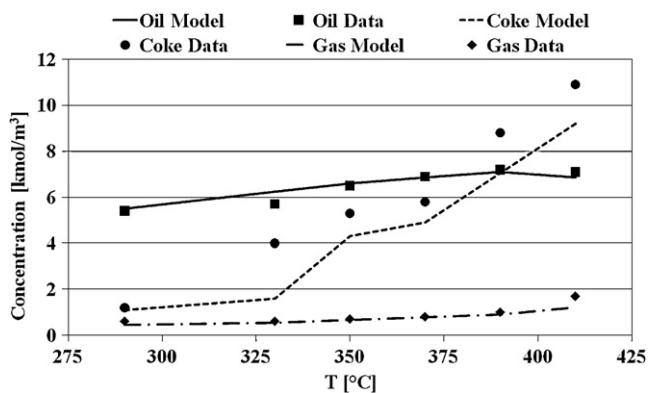

Fig. 11. Fit between a kinetic model for zeolite cracking of bio-oil and experimental data. Experiments were performed in a fixed bed reactor with aspen bio-oil as feed and HZSM-5 as catalyst. The figure is reproduced from Adjaye and Bakhshi [52].

5.3. Deactivation

As for HDO, carbon deposition and thereby catalyst deactivation constitute a pronounced problem in zeolite cracking.

In zeolite cracking, carbon is principally formed through polymerization and polycondensation reactions, such formation results in the blockage of the pores in the zeolites [143,148]. Guo et al. [148] investigated the carbon precursors formed during operation of bio-oil over HZSM-5 and found that deactivation was caused by an initial build-up of high molecular weight compounds, primarily having aromatic structures. These species formed in the inner part of the zeolites and then expanded, resulting in the deactivation of the catalyst.

Gayubo et al. [147] investigated the carbon formed on HZSM-5 during operation with synthetic bio-oil in a fixed bed reactor at 400–450 °C with temperature programmed oxidation (TPO) and found two types of carbon: thermal carbon and catalytic carbon. The thermal carbon was described as equivalent to the depositions on the reactor walls and this was only found in the macropores of the catalyst. The catalytic carbon was found in the micropores of the zeolites and was ascribed to dehydrogenation, condensation, and hydrogen transfer reactions. This was found to have a lower hydrogen content compared to the thermal carbon [147,155]. In the TPO, the thermal carbon was removed at lower temperatures (450–480 °C) compared to the catalytic carbon, which was removed at 520–550 °C. These observations were assumed due to the catalytic carbon being steric hindered, deposited in the micropores, strongly bound to the acidic sides of the zeolite, and less reactive due to the hydrogen deficient nature. The conclusion of the study was that the catalytic carbon was the principal source of deactivation, as this resulted in blockage of the internal acidic sites of the catalyst, but thermal carbon also contributed to the deactivation.

The study of Huang et al. [143] described that acid sites played a significant role in the formation of carbon on the catalysts. Proton donation from these was reported as a source for hydrocarbon cations. These were described as stabilized on the deprotonated basic framework of the zeolite, which facilitated potential for cracking and aromatization reactions, leading to carbon.

Summarizing, it becomes apparent that carbon forming reactions are driven by the presence of acid sites on the catalyst leading to poly (aromatic) carbon species. The acid sites are therefore the essential part of the mechanism for both the deoxygenating reactions (cf. Section 5.1) and the deactivating mechanisms.

Trying to decrease the extent of carbon formation on the catalyst, Zhu et al. [154] investigated co-feeding of hydrogen to anisole over HZSM-5 in a fixed bed reactor at 400 °C. This showed that the presence of hydrogen only decreased the carbon formation slightly. It was suggested that the hydrogen had the affinity to react with adsorbed carbenium ions to form paraffins, but apparently the effect of this was not sufficient to increase the catalyst lifetime in any significant degree. Ausavasukhi et al. [156] reached a similar conclusion in another study of deoxygenation of benzaldehyde over HZSM-5, where it was described that the presence of hydrogen did not influence the conversion. However, a shift in selectivity was observed as an increase in toluene production was observed with H_2, which was ascribed to hydrogenation/hydrogenolysis reactions taking place.

In a study of Peralta et al. [157] co-feeding of hydrogen was investigated for cracking of benzaldehyde over NaX zeolites with and without Cs at 475 °C. The observed conversion as a function of time on stream is shown in Fig. 12. Comparing the performance of CsNaX and NaX in hydrogen shows that the stability of the CsNaX catalyst was significantly higher as the conversion of this catalyst only decreased by ca. 10% after 8 h, compared to a drop of ca. 75% for NaX. However, as CsNaX has an initial conversion of 100% this drop
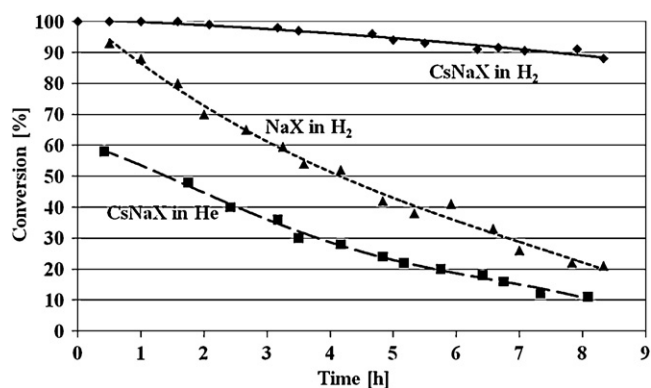
Fig. 12. Stability of CsNaX and NaX zeolites for cracking of benzaldehyde with either H_2 or He as carrier gas. Experiments were performed in a fixed bed reactor at 475 °C. Data are from Peralta et al. [157].

might not display the actual drop in activity as an overpotential might be present in the beginning of the experiment.

Replacing H_2 with He showed a significant difference for the CsNaX catalyst, as a much faster deactivation was observed in this case; dropping by ca. 90% over 8 h of operation. It was concluded that H_2 effectively participated in hydrogen transfer reactions over these catalysts, leading to the better stability. Ausavasukhi et al. [156] reported that when using HZSM-5 promoted with gallium for deoxygenation of benzaldehyde in the presence of H_2, the gallium served as hydrogen activating sites, which participated in hydrogenation reactions on the catalyst. Comparing these results to the work by Zhu et al. [154] shows that co-feeding of hydrogen over zeolites has a beneficial effect if a metal is present.

In another approach, Zhu et al. [154] showed that if water was added to an anisole feed and treated over HZSM-5 at 400 °C, the conversion was ca. 2.5 times higher than without water. It was concluded that water actively participated in the reactions on the zeolite. A possible explanation for these observations could be that low partial pressures of steam result in the formation of so called extra-framework alumina species which give an enhanced acidity and cracking activity [158,159,192]. Thus, it appears that addition of water to the system can have a beneficial effect and constitute a path worth elucidating further, but it should also be kept in mind that bio-oil already has a high water content.

In summary, the results of Zhu et al. [154], Ausavasukhi et al. [156], and Peralta et al. [157] show that a hydrogen source in catalytic cracking has a positive effect on the stability of the system. Thus, it seems that a potential exist for catalysts which are combinations of metals and zeolites and are co-fed with hydrogen. Some initial work has recently been performed by Wang et al. [160] where Pt on ZSM-5 was investigated for HDO of dibenzofuran, but generally this area is unexamined.

Finally, regeneration of zeolite catalysts has been attempted. Vitolo et al. [141] investigated regeneration of a HZSM-5 catalyst which had been operated for 60–120 min in a fixed bed reactor at 450 °C fed with bio-oil. The catalyst was washed with acetone and heated in an oven at 500 °C over 12 h. Nevertheless, a lower catalyst lifetime and deoxygenation degree was found for the regenerated catalyst relative to the fresh. This effect became more pronounced as a function of regeneration cycles. This persistent deactivation was evaluated as being due to a decrease in the availability of acid sites, which decreased by 62% over 5 regeneration cycles.

Guo et al. [130] tried to regenerate HZSM-5 at 600 °C over 12 h; the catalyst had been used in a fixed bed reactor with bio-oil as feed at 380 °C. Unfortunately the time on stream was not reported. Testing of the catalyst after regeneration showed an increasing oxygen content in the produced oil as a function of regeneration

cycles, relative to the fresh catalyst. The fresh catalyst produced oil with 21 wt% oxygen, but after 5 regenerations this had increased to 30 wt%. It was concluded that this was due to a decrease in the amount of exposed active sites on the catalyst.

At elevated steam concentrations it has been found that aluminosilicates can undergo dealumination where the tetrahedral alumina in the zeolite frame is converted into so called partially distorted octahedral alumina atoms. These can diffuse to the outer surface of the zeolite where they are converted into octahedrally coordinated alumina atoms, which are not acidic. Overall this process will entail that the availability of acidic sites in the zeolite will decrease during prolonged exposure to elevated steam concentrations [159,161]. As Vitolo et al. [141] observed a decrease in the availability of acid sites in the zeolite used for bio-oil upgrading and because bio-oil has a general high water content, it could be speculated that dealumination is inevitably occurring during zeolite cracking of bio-oil and thus regeneration cannot be done.

Overall, the work of Vitolo et al. [141] and Guo et al. [130] are in analogy with traditional FCC where air is used to remove carbon depositions on the catalyst [162], but it appears that this method can not be applied to zeolite cracking of bio-oils. Thus, new strategies are required.

6. General aspects

The grade of the fuels produced from upgrading bio-oil is an important aspect to consider, but depending on the process conditions different product compositions will be achieved. Table 7 illustrates what can be expected for the compositions and the characteristics between raw pyrolysis oil, HDO oil, zeolite cracking oil, and crude oil (as a benchmark).

Comparing bio-oil to HDO and zeolite cracking oil, it is seen that the oxygen content after HDO and zeolite cracking is decreased. In HDO a drop to <5 wt% is seen, where zeolite cracking only decreases the oxygen content to 13–24 wt%. Therefore a larger increase in the HHV is seen through HDO compared to zeolite cracking. Furthermore, the viscosity at 50 °C ($\mu_{50°C}$) of the HDO oil is seen to decrease, which improves flow characteristics and is advantageous in further processing. The decrease in the oxygen content also affects the pH value of the oil, as this increases from ca. 3 to about 6 in HDO, i.e.

Table 7
Comparison of characteristics of bio-oil, catalytically upgraded bio-oil, and crude oil.

	Bio-oil[a]	HDO[b]	Zeolite cracking[c]	Crude oil[d]
Upgraded bio-oil				
Y_{Oil} [wt%]	100	21–65	12–28	–
$Y_{Waterphase}$ [wt%]	–	13–49	24–28	–
Y_{Gas} [wt%]	–	3–15	6–13	–
Y_{Carbon} [wt%]	–	4–26	26–39	–
Oil characteristics				
Water [wt%]	15–30	1.5	–	0.1
pH	2.8–3.8	5.8	–	–
ρ [kg/l]	1.05–1.25	1.2	–	0.86
$\mu_{50°C}$ [cP]	40–100	1–5	–	180
HHV [MJ/kg]	16–19	42–45	21–36[e]	44
C [wt%]	55–65	85–89	61–79	83–86
O [wt%]	28–40	<5	13–24	<1
H [wt%]	5–7	10–14	2–8	11–14
S [wt%]	<0.05	<0.005	–	<4
N [wt%]	<0.4	–	–	<1
Ash [wt%]	<0.2	–	–	0.1
H/C	0.9–1.5	1.3–2.0	0.3–1.8	1.5–2.0
O/C	0.3–0.5	<0.1	0.1–0.3	≈0

[a] Data from [10,11,28].
[b] Data from [16,53].
[c] Data from [130,127].
[d] Data from [10,11,28].
[e] Calculated on the basis of Eq. (27) [181].

Table 8
Carbon deposition on different catalysts after operation, given in wt% of total catalyst mass. Data for zeolites in rows 1 and 2 are from Park et al. [144], experiments performed in a packed bed reactor at 500 °C over a period of 1 h with pine bio-oil. Data for HDO catalysts in rows 3 and 4 are from Gutierrez et al. [66], experiments performed in a batch reactor at 300 °C over a period of 4 h with guaiacol.

Catalyst	Carbon [wt%]
HZSM-5	13.6
Meso-MFI	21.3
Co–MoS$_2$/Al$_2$O$_3$	6.7
Rh/ZrO$_2$	1.8

making it almost neutral. Generally, the characteristics of the HDO oil approaches the characteristics of the crude oil more than those of the zeolite cracking oil.

Table 7 includes a comparison between the product distribution from HDO and zeolite cracking. Obviously, yields from the two syntheses are significantly different. The principal products from HDO are liquids, especially oil. On the contrary, the main product from zeolite cracking appears to be carbon, which constitutes a significant problem. The low oil yield from zeolite cracking further contains a large elemental fraction of oxygen. For this reason the fuel characteristics of the HDO oil is significantly better, having a HHV of 42–45 MJ/kg compared to only 21–36 MJ/kg for the zeolite cracking oil. Note, however that part of the increase in the HHV of the HDO oil is due to the addition of hydrogen. Overall, HDO oil can be produced in a larger yield and in a higher fuel grade compared to zeolite cracking oil.

A general concern in both processes is the carbon deposition. Table 8 summarizes observed carbon deposition on catalytic systems for both HDO and zeolite cracking after operation. Despite different experimental conditions it is apparent that the extent of carbon formation is more pronounced in zeolite cracking relative to HDO. To give an idea of the extent of the problem; lifetimes of around 100 h for Pd/C catalysts for HDO of bio-oil in a continuous flow setup at 340 °C were reported by Elliott et al. [61] and other studies have indicated lifetimes of around 200 h for HDO of bio-oil with Co–MoS$_2$/Al$_2$O$_3$ catalysts [43]. For zeolite cracking, Vitolo et al. [141] reported that significant deactivation of HZSM-5 occurred after only 90 min of operation in a continuous flow setup with pine bio-oil at 450 °C due to carbon deposition. Zhu et al. [154] showed that cracking of anisole with HZSM-5 in a fixed bed reactor at 400 °C caused significant deactivation over periods of 6 h. Thus, rapid deactivation is found throughout the literature, where deactivation of zeolite cracking catalysts is more pronounced than that of HDO catalysts.

Baldauf et al. [70] investigated direct distillation of HDO oil (with ca. 0.6 wt% oxygen). The produced gasoline fraction had an octane number (RON) of 62, which is low compared to 92–98 for commercial gasoline. The diesel fraction had a cetane number of 45, also being low compared to a minimum standard of 51 in Europe [163]. The overall conclusion of this study therefore was that the fuel product was not sufficient for the current infrastructure. Instead it has been found that further processing of both HDO oil and zeolite cracking is needed for production of fuel; as for conventional crude oil [125,164].

Processing of HDO oil in fluid catalytic cracking (FCC) both with and without co-feeding crude oil has been done. This approach allows on to convert the remaining oxygen in the HDO oil to CO$_2$ and H$_2$O [60,165]. Mercader et al. [60] found that if HDO oil was fed in a ratio of 20 wt% HDO oil to 80 wt% crude oil to a FCC unit, a gasoline fraction of above 40 wt% could be obtained, despite an oxygen content of up to 28 wt% in the HDO oil. The gasoline fraction proved equivalent to the gasoline from pure crude oil. Furthermore, FCC processing of pure HDO oil was found to produce gasoline

Table 9
Oil composition on a water-free basis in mol% through the bio-oil upgrading process as specified by Elliott et al. [26]. The bio-oil was a mixed wood bio-oil. HDO was performed at 340 °C, 138 bar and a LHSV of 0.25 with a Pd/C catalyst. Hydrocracking was performed at 405 °C, 103 bar and a LHSV of 0.2 with a conventional hydrocracking catalyst.

	Bio-oil	HDO oil	Hydrocracked oil
Ketones/aldehydes	13.77	25.08	0
Alkanes	0	4.45	82.85
Guaiacols etc.	34.17	10.27	0
Phenolics	10.27	18.55	0
Alcohols	3.5	5.29	0
Aromatics	0	0.87	11.53
Acids/esters	19.78	25.21	0
Furans etc.	11.68	6.84	0
Unknown	6.83	3.44	5.62

fractions equivalent to conventional gasoline, with oxygen content in the HDO oil up to ca. 17 wt% [60].

Elliott et al. [26] investigated upgrading of HDO oil through conventional hydrocracking and found that by treating the HDO oil at 405 °C and 100 bar with a conventional hydrocracking catalyst the oxygen content in the oil decreased to less than 0.8 wt% (compared to 12–18 wt% in the HDO oil). In Table 9 the development in the oil composition through the different process steps can be seen. From bio-oil to HDO oil it is seen that the fraction of larger oxygen containing molecules decreases and the fraction of the smaller molecules increases. Through the hydrocracking the smaller oxygen containing molecules is converted, in the end giving a pure hydrocarbon product. The process was reported to have an overall yield of 0.33–0.64 g oil per g of bio-oil.

7. Prospect of catalytic bio-oil upgrading

The prospect of catalytic bio-oil upgrading should be seen not only in a laboratory perspective, but also in an industrial one. Fig. 13 summarizes the outline of an overall production route from biomass to liquid fuels through HDO. The production is divided into two sections: flash pyrolysis and biorefining.

In the pyrolysis section the biomass is initially dried and grinded to reduce the water content and produce particle sizes in the range of 2–6 mm, which are needed to ensure sufficiently fast heating during the pyrolysis. The actual pyrolysis is here occurring as a circulating fluid bed reactor system where hot sand is used as heating source, but several other routes also exists [9,29,31,32,38,166]. The sand is subsequently separated in a cyclone, where the biomass vapour is passed on in the system. By condensing, liquids and residual solids are separated from the incondensable gases. The oil and solid fraction is filtered and the bio-oil is stored or sent to another processing site. The hot off-gas from the condenser is passed on to a combustion chamber, where methane, and potentially other hydrocarbons, is combusted to heat up the sand for the pyrolysis. The off-gas from this combustion is in the end used to dry the biomass in the grinder to achieve maximum heat efficiency.

For a company to minimize transport costs, bio-oil production should take place at smaller plants placed close to the biomass source and these should supply a central biorefinery for the final production of the refined bio-fuel. This is illustrated in Fig. 13 by several trucks supplying feed to the biorefinery section. In this way the bio-refinery plant is not required to be in the immediate vicinity of the biomass source (may be >170 km), as transport of bio-oil can be done at larger distances and still be economically feasible [39,40].

At the biorefinery plant the bio-oil is fed to the system and initially pressurized and heated to 150–280 °C [75,104]. It has been proposed to incorporate a thermal treatment step without catalyst prior to the catalytic reactor with either the HDO or zeolite
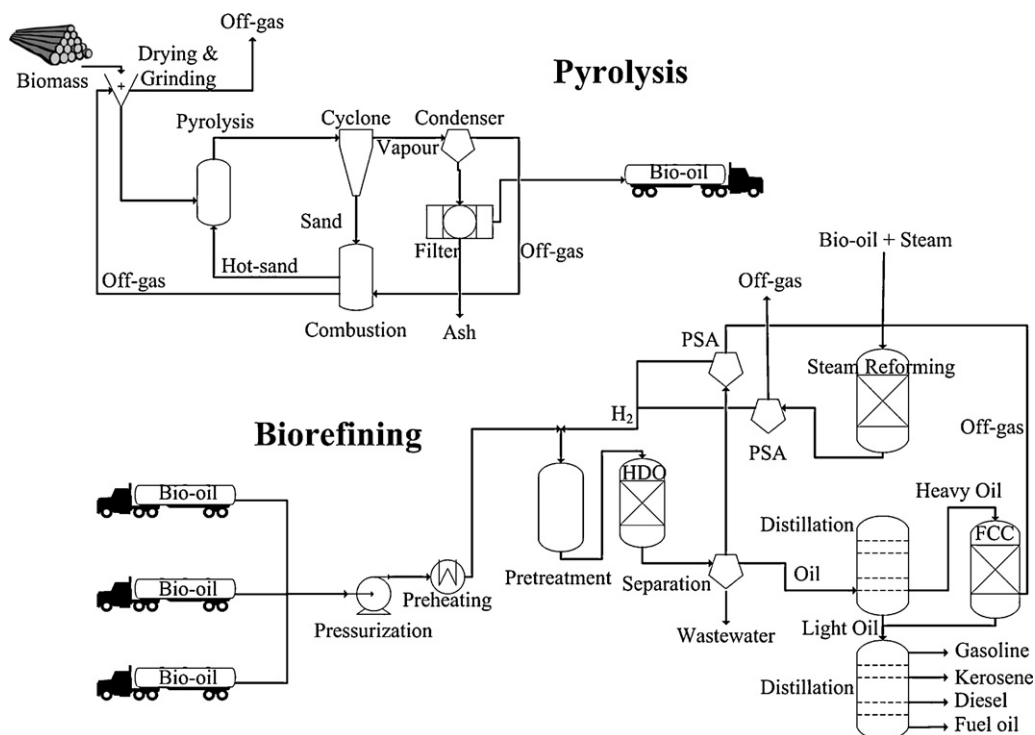
Fig. 13. Overall flow sheet for the production of bio-fuels on the basis of catalytic upgrading of bio-oil. The figure is based on information from Jones et al. [167].

catalyst. This should take place between 200 and 300 °C and can be carried out both with and without the presence of hydrogen. This will prompt the reaction and stabilization of some of the most reactive compounds in the feed and thereby lower the affinity for carbon formation in downstream processes [11,75,159,164,167]. After the thermal treatment the actual HDO synthesis is prompted, producing oils equivalent to the descriptions of Table 7.

The HDO oil is processed by an initial distillation to separate light and heavy oil. The heavy oil fraction is further processed through cracking, which here is illustrated by FCC, but also could be hydrocracking. The cracked oil fraction is hereafter joined with the light oil fraction again. Finally, distillation of the light oil is performed to separate gasoline, diesel, etc.

Off-gasses from the HDO and the FCC should be utilised in the hydrogen production. However, these are not sufficient to produce the required amount of hydrogen for the synthesis, instead additional bio-oil (or another feed) should be supplied to the plant [167]. In the flow sheet of Fig. 13, steam reforming is shown simplified as a single step followed by hydrogen separation through pressure swing adsorption (PSA). In reality this step is more complex, as heat recovery, feed pre-treatment, and water-gas-shift all would have to be incorporated in such a section, but these details are outside the scope of this study, readers should instead consult references [168–171]. If hydrogen is supplied from steam reforming of bio-oil, as indicated in Fig. 13, it would result in a decrease in the fuel production from a given amount of bio-oil by about one third [167]. In the future it is believed that the hydrogen could be supplied through hydrolysis with energy generation on the basis of solar or wind energy, when these technologies are mature [57,172,173]. This also offers a route for storage of some of the solar energy.

In between the pyrolysis and the HDO plant a potential stabilization step could be inserted due to the instability of the bio-oil. The necessity of this step depends on a series of parameters: the time the bio-oil should be stored, the time required for transport, and the apparent stability of the specific bio-oil batch. The work of Oasmaa and Kuoppala [50] indicates that utilisation of the bio-oil should be

done within three months if no measures are taken. Different methods have been suggested in order to achieve increased stability of bio-oil; one being mixing of the bio-oil with alcohols, which should decrease the reactivity [49,152,159]. Furthermore a low temperature thermal hydrotreatment (100–200 °C) has been proposed, as this will prompt the hydrodeoxygenation and cracking of some of the most reactive groups [23].

In the design of a catalytic upgrading unit it is relevant to look at the already well established HDS process, where the usual choice is a trickle bed reactor [9,120,174,175]. Such a reactor is illustrated in Fig. 14. This is essentially a packed bed reactor, but operated in a multiphase regime. In the reactor the reactions occur between the dissolved gas (hydrogen) and the liquid on the catalytic surface. The liquid flow occurs as both film and rivulet flow filling the catalyst pores with liquid [176,177]. The advantages of using a trickle bed reactor, with respect to the current HDO process, are: the flow pattern resemblance plug flow behaviour giving high conversions, low catalyst loss, low liquid/solid ratio ensuring low affinity for homogenous reactions in the oil, relatively low investment costs, and possibility to operate at high pressure and temperature [177,175].

The HDO process has been evaluated as being a suitable choice in the production of sustainable fuels, due to a high carbon efficiency and thereby a high production potential [10,23,173,178]. In an evaluation by Singh et al. [173] it was estimated that the production capacity on an arable land basis was 30–35 MJ fuel/m^2 land/year for pyrolysis of the biomass followed by HDO, combined with gasification of a portion of the biomass for hydrogen production. In comparison, gasification of biomass followed by Fischer–Tropsch synthesis was in the same study estimated as having a land utilisation potential in the order of 21–26 MJ fuel/m^2 land/y. It was further found that the production of fuels through HDO could be increased by approximately 50% if the hydrogen was supplied from solar energy instead of gasification, thus being 50 MJ fuel/m^2 land/year. However, care should be taken with these results, as they are calculated on the basis of assumed achievable process efficiencies.
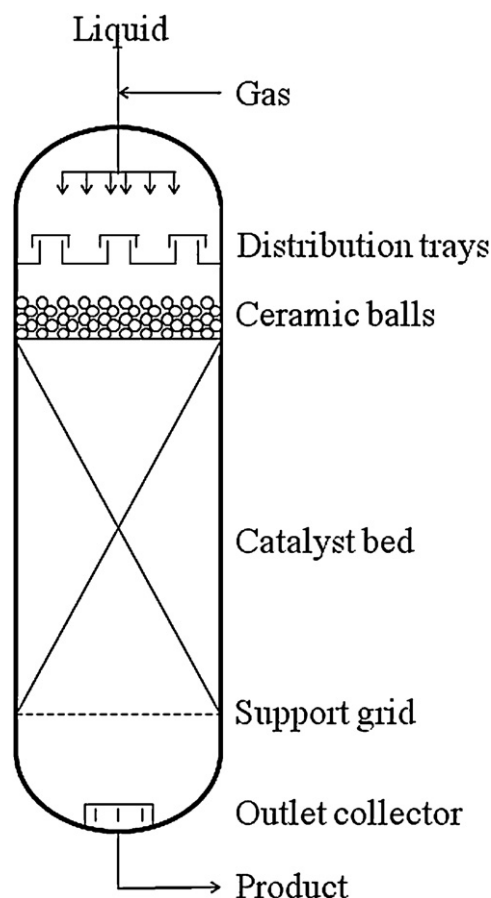
Fig. 14. Scheme of a trickle bed reactor. The figure is drawn on the basis of information from Mederos et al. [175].

A relatively new economic study has been made by the U. S. Department of Energy [167] where all process steps were taken into consideration, in analogy to Fig. 13, but with natural gas as hydrogen source. The total cost from biomass to gasoline was calculated to be 0.54 $/l of gasoline, compared to a price of 0.73 $/l for crude oil derived gasoline in USA at present, excluding distribution, marketing, and taxes [179]. Thus, this work concluded that production of fuels through the HDO synthesis is economically feasible and cost-competitive with crude oil derived fuels. However, a certain uncertainty in the calculated price of the synthetic fuel must be remembered and the reported value is therefore not absolute.

The above discussion only treats the production and prices of the HDO synthesis. To the knowledge of the authors, zeolite cracking has not yet been evaluated as an industrial scale process.

Evaluating zeolite cracking in industrial scale would include some changes relative to Fig. 13, with the exclusion of hydrogen production as the most evident. Alternatively, the zeolite cracking could be placed directly after the pyrolysis reactor, treating the pyrolysis vapours online [127,144,149,180]. Hong-yu et al. [149] concluded that online upgrading was superior in liquid yield and further indicated that a better economy could be achieved this way, compared to the two separate processes. However, oxygen content was reported as being 31 wt% in the best case scenario, indicating that other aspects of zeolite cracking still should be elucidated prior to evaluating the process in industrial scale.

8. Discussion

Catalytic bio-oil upgrading is still a technology in its infancy regarding both HDO and zeolite cracking. Zeolite cracking is the most attractive path due to more attractive process conditions, in terms of the low pressure operation and independence of hydrogen feed and this could make it easy to implement in industrial scale. However, the high proportion of carbon formed in the process deactivates the zeolites, presently giving it insufficient lifetime. Another concern is the general low grade of the fuel produced, as shown in Table 7. Explicitly, the low heating value entails that the produced fuel will be of a grade too low for utilisation in the current infrastructure. Increasing this low fuel grade does not seem possible, as the effective H/C ratio calculated from Eq. (18) at maximum can be 0.6; significantly lower than the typical value of crude oil (1.5–2). Furthermore, zeolite cracking has proven unable to give high degrees of deoxygenation, as O/C ratios of 0.6 in the product have been reported (compared to 0 of crude oil). Low H/C ratios and high O/C ratios both contribute to low heating values, as seen from Channiwala's and Parikh's correlation for calculation of the HHV on the basis of the elemental composition in wt% [181]:

$$HHV\,[MJ/kg] = 0.349 \cdot C + 1.178 \cdot H - 0.103 \cdot O - 0.015 \cdot N$$
$$+ 0.101 \cdot S - 0.021 \cdot ash \qquad (27)$$

Here it is seen that hydrogen contributes positively and oxygen negatively.

We conclude that zeolite cracking can not produce fuels of sufficient quality to cope with the demands in the current infrastructure. This is in agreement with Huber et al. [16] where the usefulness of the technology was questioned due to the low hydrocarbon yields and high affinity for carbon formation. Zhang et al. [28] expressed concern about the low quality of the fuels, concluding that zeolite cracking was not a promising route for bio-oil upgrading.

The process still seems far from commercial industrial application in our point of view. To summarize, three crucial aspects still has to be improved: product selectivity (oil rather than gas and solids), catalyst lifetime, and product quality.

Overall it is concluded that a hydrogen source is a requirement in order to upgrade bio-oil to an adequate grade fuel, i.e. HDO. However, this route is also far from industrial application. A major concern of this process is the catalyst lifetime, as carbon deposition on these systems has to be solved before steady production can be achieved.

Regarding deactivation mechanisms it appears that sulphur poisoning from the bio-oil has been disregarded so far, as carbon has been a larger problem and because much effort has been focused on the sulphur tolerant Co–MoS$_2$ and Ni–MoS$_2$ systems. However, a number of interesting catalysts for hydrodeoxygenation of bio-oil not based on CoMo and NiMo hydrotreating catalysts have been reported recently. With the work by Thibodeau et al. [182], Wildschut et al. [53,104,183,184], Elliott et al. [61], and Yakovlev et al. [98,185,186] a turn toward new catalysts such as WO$_3$, Ru/C, Pd/C, or NiCu/CeO$_2$ has been indicated. Drawing the parallel to steam reforming where some of these catalysts have been tested, it is well known that even low amounts of sulphur over e.g. a nickel catalyst will result in deactivation of the catalyst [187–189]. As bio-oil is reported to contain up to 0.05 wt% sulphur, deactivation of such catalytic systems seems likely.

Other challenges of HDO involve description of the kinetics, which so far has been limited to either lumped models or compound specific models. Neither of these approaches seems adequate for any general description of the system and therefore much benefit can still be obtained in clarifying the kinetics. Inspiration can be found when comparing to already well established hydrotreating processes, such as HDS and hydrocracking. In industry these systems are described on the basis of a pseudo component approach, where the feed is classified on the basis of either boiling range or hydrocarbon type. In this way the kinetic model treats the kinetics

of the individual fractions on the basis of detailed kinetic investigations on representative model compounds [190,191]. In order to describe the kinetics of HDO (and zeolite cracking as well) of bio-oil an approach similar to this would probably be necessary, where the division probably should be on the basis of functional groups.

Further elucidation of HDO in industrial scale is also a request. Elaboration of why high pressure operation is a necessity and evaluation of potential transport limitations in the system are still subjects to be treated, they also have been questioned by Venderbosch et al. [11]. Both aspects affect the reactor choice, as the proposed trickle bed reactor in Section 7 potentially could be replaced with a better engineering solution.

9. Conclusion and future tasks

Due to the demand for fuels, the increased build-up of CO_2 in the atmosphere, and the general fact that the oil reserves are depleting, the need of renewable fuels is evident. Biomass derived fuels is in this context a promising route, being the only renewable carbon resource with a sufficiently short reproduction cycle.

Problems with biomass utilisation are associated with the high cost of transport due to the low mass and energy density. To circumvent this, local production of bio-oil seems a viable option, being a more energy dense intermediate for processing of the biomass. This process is further applicable with all types of biomass. However, the bio-oil suffers from a high oxygen content, rendering it acidic, instable, immiscible with oil, and giving it a low heating value. Utilisation of bio-oil therefore requires further processing in order to use it as a fuel.

Several applications of bio-oil have been suggested. Deoxygenation seems one of the most prospective options, which is a method to remove the oxygen containing functional groups. Two different main routes have been proposed for this: HDO and zeolite cracking.

HDO is a high pressure synthesis where oxygen is removed from the oil through hydrogen treatment. This produces oil with low oxygen content and a heating value equivalent to crude oil.

Zeolite cracking is performed at atmospheric pressure in the absence of hydrogen, removing oxygen through cracking reactions. This is attractive from a process point of view, but it has been found unfeasible since the product is a low grade fuel and because of a too high carbon formation (20–40 wt%). The latter results in rapid deactivation of the catalyst.

Overall HDO seems the most promising route for production of bio-fuels through upgrading of bio-oil and the process has further been found economically feasible with production prices equivalent to conventional fuels from crude oil, but challenges still exist within the field. So far the process has been evaluated in industrial scale to some extent, elucidating which unit operations should be performed when going from biomass to fuel. However, aspects of the transport mechanisms in the actual HDO reactor and the high pressure requirement are still untreated subjects which could help optimize the process and bring it closer to industrial utilisation. Another great concern within the field is catalyst formulation. Much effort has focused around either the Co–MoS_2 system or noble metal catalysts, but due to a high affinity for carbon formation, and also due to the high raw material prices for the noble metals, alternatives are needed. Thus, researchers investigate to substitute the sulphide catalysts with oxide catalysts and the noble catalysts with base metal catalysts. The principal requirement to catalysts are to have a high resistance toward carbon formation and at the same time have a sufficient activity in hydrodeoxygenation.

Overall the conclusion of this review is that a series of fields still have to be investigated before HDO can be used in industrial scale. Future tasks include:

- Catalyst development; investigating new formulations, also in combination with DFT to direct the effort.
- Improved understanding of carbon formation mechanism from classes of compounds (alcohols, carboxylic acids, etc.).
- Better understanding of the kinetics of HDO of model compounds and bio-oil.
- Influence of impurities, like sulphur, in bio-oil on the performance of different catalysts.
- Decrease of reaction temperature and partial pressure of hydrogen.
- Defining the requirement for the degree of oxygen removal in the context of further refining.
- Finding (sustainable) sources for hydrogen.

Acknowledgements

References

[1] United Nations Department of Economic and Social Affairs, 2010, http://www.un.org/esa/population/.
[2] U.S. Energy Information Administration Independent Statistics and Analysis, 2010, http://www.eia.doe.gov/.
[3] B. van Ruijven, D.P. van Vuuren, Energy Policy 37 (2009) 4797–4808.
[4] M. Balat, Energy Convers. Manage. 52 (2011) 858–875.
[5] S. Sorrell, J. Speirs, R. Bentley, A. Brandt, R. Miller, Energ. Policy 38 (2010) 5290–5295.
[6] R. Pachauri, A. Reisinger (Eds.), Climate change 2007: synthesis report. Contribution of working groups I, II and III to the fourth assessment report of the intergovernmental panel on climate change, Technical report, IPCC, 2007.
[7] A. Roedl, Int. J. Life Cycle Assess. 15 (2010) 567–578.
[8] BP Statistical Review of World Energy, 2010, bp.com/statisticalreview.
[9] M.F. Demirbas, Appl. Energy 88 (2011) 17–28.
[10] J. Holmgren, R. Marinageli, P. Nair, D.C. Elliott, R. Bain, Hydrocarbon Process. (2008) 95–103.
[11] R.H. Venderbosch, A.R. Ardiyanti, J. Wildschut, A. Oasmaa, H.J. Heeres, J. Chem. Technol. Biotechnol. 85 (2010) 674–686.
[12] H. Wenzel, Breaking the biomass bottleneck of the fossil free society, Technical report, Concito, 2010.
[13] P. McKendry, Bioresour. Technol. 83 (2002) 37–46.
[14] T. Damartzis, A. Zabaniotou, Renew. Sustain. Energy Rev. 15 (2011) 366–378.
[15] K. Göransson, U. Söderlind, J. He, W. Zhang, Renew. Sustain. Energy Rev. 15 (2011) 482–492.
[16] G.W. Huber, S. Iborra, A. Corma, Chem. Rev. 106 (2006) 4044–4098.
[17] M.J.A. Tijmensen, A.P.C. Faaij, C.N. Hamelinck, M.R.M. van Hardeveld, Biomass Bioeng. 23 (2002) 129–152.
[18] J.M. Christensen, P.A. Jensen, N.C. Schiødt, A.D. Jensen, ChemCatChem 2 (2010) 523–526.
[19] J.M. Christensen, P.M. Mortensen, R. Trane, P.A. Jensen, A.D. Jensen, Appl. Catal. A: Gen. 366 (2009) 29–43.
[20] F.J. Keil, Microporous Mesoporous Mater. 29 (1999) 49–66.
[21] P.L. Spath, M.K. Mann, W.A. Amos, Update of hydrogen from biomass—determination of the delivered cost of hydrogen, Technical report, U.S. Department of Energy's Hydrogen Program, 2003.
[22] M. Stöcker, Microporous Mesoporous Mater. 29 (1999) 3–48.
[23] P. Grange, E. Laurent, R. Maggi, A. Centeno, B. Delmon, Catal. Today 29 (1996) 297–301.
[24] C. Perego, A. Bosetti, Microporous Mesoporous Mater. 144 (2011) 28–39.
[25] J.G. Rogers, J.G. Brammer, Biomass Bioeng. 33 (2009) 1367–1375.
[26] D.C. Elliott, Energy Fuels 21 (2007) 1792–1815.
[27] E. Furimsky, Appl. Catal. A: Gen. 199 (2000) 144–190.
[28] Q. Zhang, J. Chang, T. Wang, Y. Xu, Energy Convers. Manage. 48 (2007) 87–92.
[29] A.V. Bridgwater, Biomass Bioeng., in press.
[30] S. Czernik, A.V. Bridgwater, Energy Fuels 18 (2004) 590–598.
[31] R.H. Venderbosch, W. Prins, Biofuels Bioprod. Biorefin. 4 (2010) 178–208.
[32] D. Mohan, C.U. Pittman, P.H. Steele, Energy Fuels 20 (2006) 848–889.
[33] D.C. Elliott, E.G. Baker, D. Beckman, Y. Solantausta, V. Tolenhiemo, S. Gevert, C. Hörnell, A. Östman, B. Kjellström, Biomass 22 (1990) 251–269.
[34] J. Akhtar, N.A.S. Amin, Renew. Sustain. Energy Rev. 15 (2011) 1615–1624.
[35] A. Demirbas, Energy Convers. Manage. 41 (2000) 633–646.
[36] J. Moffatt, R. Overend, Biomass 7 (1985) 99–123.

[37] A.A. Peterson, F. Vogel, R.P. Lachance, M. Froling, M.J. Antal, J.W. Tester, Energy Environ. Sci. 1 (2008) 32–65.
[38] T. Bridgwater, J. Sci. Food Agric. 86 (2006) 1755–1768.
[39] P.C. Badger, P. Fransham, Biomass Bioeng. 30 (2006) 321–325.
[40] K. Raffelt, E. Henrich, A. Koegel, R. Stahl, J. Steinhardt, F. Weirich, Appl. Biochem. Biotechnol. 129 (2006) 153–164.
[41] A. Demirbas, M. Balat, H. Balat, Energy Convers. Manage. 52 (2011) 1815–1828.
[42] S. Yaman, Energy Convers. Manage. 45 (2004) 651–671.
[43] A.V. Bridgwater, Catal. Today 29 (1996) 285–295.
[44] H.B. Goyal, D. Seal, R.C. Saxena, Renew. Sustain. Energy Rev. 12 (2008) 504–517.
[45] C.A. Mullen, A.A. Boateng, N.M. Goldberg, I.M. Lima, D.A. Laird, K.B. Hicks, Biomass Bioeng. 34 (2010) 67–74.
[46] L. Qiang, L. Wen-Zhi, Z. Xi-Feng, Energy Convers. Manage. 50 (2009) 1376–1383.
[47] A. Oasmaa, D.C. Elliott, J. Korhonen, Energy Fuels 24 (2010) 6548–6554.
[48] J.D. Adjaye, R.K. Sharma, N.N. Bakhshi, Fuel Process. Technol. 31 (1992) 214–256.
[49] M.E. Boucher, A. Chaala, H. Pakdel, C. Roy, Biomass Bioeng. 19 (2000) 351–361.
[50] A. Oasmaa, E. Kuoppala, Energy Fuels 17 (2003) 1075–1084.
[51] J.D. Adjaye, N.N. Bakhshi, Biomass Bioeng. 8 (1995) 131–149.
[52] J.D. Adjaye, N.N. Bakhshi, Fuel Process. Technol. 45 (1995) 161–183.
[53] J. Wildschut, F.H. Mahfud, R.H. Venderbosch, H.J. Heeres, Ind. Eng. Chem. Res. 48 (2009) 10324–10334.
[54] I. Barin, in: Thermochemical Data of Pure Substances, VCH, 1989.
[55] F.E. Massoth, P. Politzer, M.C. Concha, J.S. Murray, J. Jakowski, J. Simons, J. Phys. Chem. B 110 (2006) 14283–14291.
[56] Y. Yunquan, L. He'an, T. Gangsheng, K.J. Smith, T.C. Thian, Chin. J. Chem. Eng. 16 (2008) 733–739.
[57] A. Corma, G.W. Huber, Angew. Chem. Int. Ed. 46 (2007) 7184–7201.
[58] A.V. Bridgwater, Appl. Catal. A: Gen. 116 (1994) 5–47.
[59] J. Wildschut, Pyrolysis oil upgrading to transportation fuels by catalytic hydrotreatment, Ph.D. thesis, Rijksuniversiteit Groningen, 2009.
[60] F. de Miguel Mercader, M.J. Groeneveld, S.R.A. Kersten, N.W.J. Way, C.J. Schaverien, J.A. Hogendoorn, Appl. Catal. B: Environ. 96 (2010) 57–66.
[61] D.C. Elliott, T.R. Hart, G.G. Neuenschwander, L.J. Rotness, A.H. Zacher, Environ. Prog. 28 (2009) 441–449.
[62] A. Daudin, L. Bournay, T. Chapus, 'Us 2010/0163458 a1', Method for converting effluents of renewable origin into fuel of excellent quality by using a molybdenum-based catalyst, 2010.
[63] M.J. McCall, T.A. Brandvold, 'Us 2009/0253948 a1', Fuel and fuel blending components from biomass derived pyrolysis oil, 2009.
[64] K.C. Kwon, H. Mayfield, T. Marolla, B. Nichols, M. Mashburn, Renew. Energy 36 (2011) 907–915.
[65] J. Gagnon, S. Kaliaguine, Ind. Eng. Chem. Res. 27 (1988) 1783–1788.
[66] A. Gutierrez, R.K. Kaila, M.L. Honkela, R. Slioor, A.O.I. Krause, Catal. Today 147 (2009) 239–246.
[67] Z. Su-Ping, Y. Yong-Jie, R. Zhengwei, L. Tingchen, Energy Source 25 (2003) 57–65.
[68] A. Oasmaa, E. Kuoppala, A.R. Ardiyanti, R.H. Venderbosch, H.J. Heeres, Energy Fuels 24 (2010) 5264–5272.
[69] M. Badawi, J.-F. Paul, S. Cristol, E. Payen, Y. Romero, F. Richard, S. Brunet, D. Lambert, X. Portier, A. Popov, E. Kondratieva, J.M. Goupil, J.E. Fallah, J.-P. Gilson, L. Mariey, A. Travert, F. Mauge, J. Catal. 282 (2011) 155–164.
[70] W. Baldauf, U. Balfanz, M. Rupp, Biomass Bioeng. 7 (1994) 237–244.
[71] V. Bui, D. Laurenti, P. Delichère, C. Geantet, Appl. Catal. B: Environ. 111 (2011) 239–245.
[72] A. Centeno, E. Laurent, B. Delmon, J. Catal. 154 (1995) 288–298.
[73] M.C. Edelman, M.K. Maholland, R.M. Baldwin, S.W. Cowley, J. Catal. 111 (1988) 243–253.
[74] M. Ferrari, S. Bosmans, R. Maggi, B. Delmon, P. Grange, Catal. Today 65 (2001) 257–264.
[75] R.J. French, J. Hrdlicka, R. Baldwin, Environ. Prog. 29 (2010) 142–150.
[76] R.J. French, J. Stunkel, R.M. Baldwin, Energy Fuels 25 (2011) 3266–3274.
[77] I. Gandarias, V.L. Barrio, J. Requies, P.L. Arias, J.F. Cambra, M.B. Güemez, Int. J. Hydrogen Energy 33 (2008) 3485–3488.
[78] R. Nava, B. Pawelec, P. Castaño, M.C. Álvarez Galván, C.V. Loricera, J.L.G. Fierro, Appl. Catal. B: Environ. 92 (2009) 154–167.
[79] E.-M. Ryymin, M.L. Honkela, T.-R. Viljava, A.O.I. Krause, Appl. Catal. A: Gen. 358 (2009) 42–48.
[80] E.-M. Ryymin, M.L. Honkela, T.-R. Viljava, A.O.I. Krause, Appl. Catal. A: Gen. 389 (2010) 114–121.
[81] M.C. Samolada, W. Baldauf, I.A. Vasalos, Fuel 77 (1998) 1667–1675.
[82] T.-R. Viljava, R.S. Komulainen, A.O.I. Krause, Catal. Today 60 (2000) 83–92.
[83] W. Zhang, Y. Zhan, L. Zhao, W. Wei, Energy Fuels 24 (2010) 2052–2059.
[84] M. Badawi, S. Cristol, J.-F. Paul, E. Payen, C. R. Chimie 12 (2009) 754–761.
[85] Y. Romero, F. Richard, S. Brunet, Appl. Catal. B: Environ. 98 (2010) 213–223.
[86] H. Topsøe, B.S. Clausen, F.E. Massoth, in: Hydrotreating Catalysysis, Springer-Verlag, 1996.
[87] O. Senol, E.-M. Ryymin, T.-R. Viljava, A. Krause, J. Mol. Catal. A: Chem. 277 (1/2) (2007) 107–112, http://www.sciencedirect.com/science/article/B6TGM-4P8B127-2/2/682438c2437b564a1ba52d249082eb09.
[88] O. Senol, T.-R. Viljava, A. Krause, Appl. Catal. A: Gen. 326 (2) (2007) 236–244, http://www.sciencedirect.com/science/article/B6TF5-4NJ7W8M-1/2/59c30bf5dd19d34130728b3e46c13f91.
[89] R. Prins, in: Handbook of Heterogeneous Catalysis, Wiley, 2008, pp. 2695–2718 (chapter 13.2).
[90] D.R. Moberg, T.J. Thibodeau, F.G. Amar, B.G. Frederick, J. Phys. Chem. C 114 (2010) 13782–13795.
[91] A. Gervasini, A. Auroux, J. Catal. 131 (1991) 190–198.
[92] S. Li, D.A. Dixon, J. Phys. Chem. A 110 (2006) 6231–6244.
[93] V.M.L. Whiffen, K.J. Smith, Energy Fuels 24 (2010) 4728–4737.
[94] S. Echeandia, P.L. Arias, V.L. Barrio, B. Pawelec, J.L.G. Fierro, Appl. Catal. B: Environ. 101 (2010) 1–12.
[95] M.J. Mendes, O.A.A. Santos, E. Jordão, A.M. Silva, Appl. Catal. A: Gen. 217 (2001) 253–262.
[96] A.Y. Stakheev, L.M. Kustov, Appl. Catal. A: Gen. 188 (1999) 3–35.
[97] M.A. Vannice, B. Sen, J. Catal. 115 (1989) 65–78.
[98] V.A. Yakovlev, S.A. Khromova, O.V. Sherstyuk, V.O. Dundich, D.Y. Ermakov, V.M. Novopashina, M.Y. Lebedev, O. Bulavchenko, V.N. Parmon, Catal. Today 144 (2009) 362–366.
[99] T. Mallat, A. Baiker, Appl. Catal. A: Gen. 200 (2000) 3–22.
[100] A. Vargas, T. Bürgi, A. Baiker, J. Catal. 222 (2004) 439–449.
[101] A. Vargas, S. Reimann, S. Diezi, T. Mallat, A. Baiker, J. Mol. Catal. 282 (2008) 1–8.
[102] S.D. Lin, D.K. Sanders, M.A. Vannice, Appl. Catal. A: Gen. 113 (1994) 59–73.
[103] M.A. Vannice, Catal. Today 12 (1992) 255–267.
[104] J. Wildschut, J. Arentz, C.B. Rasrendra, R.H. Venderbosch, H.J. Heeres, Environ. Prog. 28 (2009) 450–460.
[105] C.A. Fisk, T. Morgan, Y. Ji, M. Crocker, C. Crofcheck, S.A. Lewis, Appl. Catal. A: Gen. 358 (2009) 150–156.
[106] U.S. Geological Survey, Mineral Commodity Summaries 2010, 2010, http://minerals.usgs.gov/minerals/pubs/mcs/.
[107] H.Y. Zhao, D. Li, P. Bui, S.T. Oyama, Appl. Catal. A: Gen. 391 (2010) 305–310.
[108] C. Zhao, J. He, A.A. Lemonidou, X. Li, J.A. Lercher, J. Catal. 280 (2011) 8–16.
[109] C. Zhao, Y. Kuo, A.A. Lemonidou, X. Li, J.A. Lercher, Angew. Chem. Int. Ed. 48 (2009) 3987–3990.
[110] C. Zhao, Y. Kuo, A.A. Lemonidou, X. Li, J.A. Lercher, Chem. Commun. 46 (2010) 412–414.
[111] E. Laurent, B. Delmon, J. Catal. 146 (1994) 281–291.
[112] A. Popov, E. Kondratieva, J.M. Goupil, L. Mariey, P. Bazin, J.-P. Gilson, A. Travert, F. Mauge, J. Phys. Chem. C 114 (2010) 15661–15670.
[113] K.V.R. Charry, H. Ramakrishna, G. Murali Dhar, J. Mol. Catal. 68 (1991) L25–L30.
[114] D.C. Elliott, T.R. Hart, Energy Fuels 23 (2009) 631–637.
[115] R. Maggi, B. Delmon, Stud. Surf. Sci. Catal. 106 (1997) 99–113.
[116] A. Popov, E. Kondratieva, J.-P. Gilson, L. Mariey, A. Travert, F. Mauge, IR study of the interaction of phenol with oxides and sulfided CoMo catalysts for bio-fuels hydrodeoxygenation, Catal. Today 172 (2011) 132–135.
[117] V. Bui, D. Laurenti, P. Delichère, C. Geantet, Appl. Catal. B: Environ. 111 (2011) 246–255.
[118] V.O. Dundich, S.A. Khromova, D.Y. Ermakov, M.Y. Lebedev, V.M. Novopashina, V.G. Sister, A.I. Yakimchuk, V.A. Yakovlev, Kinet. Catal. 51 (2010) 728–734.
[119] Y.E. Sheu, R.G. Anthony, E.J. Soltes, Fuel Process. Technol. 19 (1988) 31–50.
[120] E. Furimsky, F.E. Massoth, Catal. Today 52 (1999) 381–495.
[121] A. Fonseca, P. Zeuthen, J. Nagy, Fuel 75 (1996) 1413–1423.
[122] A. Fonseca, P. Zeuthen, J. Nagy, Fuel 75 (1996) 1363–1376.
[123] S.M. Richardson, H. Nagaishi, M.R. Gray, Proceedings of the 210th National Meeting of the American Chemical Society, vol. 40, 1995, pp. 455–459.
[124] Y. Yamamoto, F. Kumata, F.E. Massoth, Fuel Process. Technol. 19 (1988) 253–263.
[125] S.R.A. Kersten, W.P.M. van Swaaij, L. Lefferts, K. Seshan, in: Catalysis for Renewables: From Feedstock to Energy Production, Wiley, 2007, pp. 119–146 (chapter 6).
[126] J.D. Adjaye, N.N. Bakhshi, Biomass Bioeng. 8 (1995) 265–277.
[127] P.T. Williams, P.A. Horne, Biomass Bioeng. 7 (1994) 223–236.
[128] S. Vitolo, M. Seggiani, P. Frediani, G. Ambrosini, L. Polit, Fuel 78 (1999) 1147–1159.
[129] N.Y. Chen, J.T.F. Degnan, L.R. Koenig, Chem. Tech. 16 (1986) 506–511.
[130] X. Guo, Y. Yan, T. Li, Chin. J. Chem. Eng. 4 (2004) 53–58.
[131] M. Balat, M. Balat, E. Kirtay, H. Balat, Energy Convers. Manage. 50 (2009) 3147–3157.
[132] M. Stöcker, Microporous Mesoporous Mater. 82 (2005) 257–292.
[133] J.M. Thomas, R.G. Bell, C.R.A. Catlow, in: Handbook of Heterogeneous Catalysis, Wiley-VCH Verlag, 1997, pp. 286–310 (chapter 2.3).
[134] H. van Bekkum, E.M. Flanigen, P.A. Jacobs, J.C. Jansen, in: Introduction to Zeolite Science and Practice, Elsevier, 2001.
[135] J. Weitkamp, Solid State Ionics 131 (2000) 175–188.
[136] R. Xu, W. Pang, J. Yu, Q. Huo, J. Chen, in: Structural Chemistry of Microporous Material, John Wiley & Sons, 2007, pp. 19–116 (chapter 2).
[137] R. Xu, W. Pang, J. Yu, Q. Huo, J. Chen, in: Chemisty of Zeolites and Related Porous Material, John Wiley & Sons, 2007, pp. 345–396 (chapter 6).
[138] A. Corma, G.W. Huber, L. Sauvanaud, P. O'Connor, J. Catal. 247 (2007) 307–327.
[139] H. Chiang, A. Bhan, J. Catal. 271 (2010) 251–261.
[140] J.D. Adjaye, N.N. Bakhshi, Biomass Bioeng. 7 (1994) 201–211.
[141] S. Vitolo, B. Bresci, M. Seggiani, M.G. Gallo, Fuel 80 (2001) 17–26.
[142] P. Dejaifve, J.C. Védrine, V. Bolis, E.G. Derouane, J. Catal. 63 (1980) 331–345.
[143] J. Huang, W. Long, P.K. Agrawal, C.W. Jones, J. Phys. Chem. C 113 (2009) 16702–16710.

[144] H.J. Park, H.S. Heo, J.-K. Jeon, J. Kim, R. Ryoo, K.-E. Jeong, Y.-K. Park, Appl. Catal. B: Environ. 95 (2010) 365–373.
[145] J.D. Adjaye, N.N. Bakhshi, Fuel Process. Technol. 45 (1995) 161–183.
[146] A.G. Gayubo, A.T. Aguayo, A. Atutxa, B. Valle, J. Bilbao, J. Chem. Technol. Biotechnol. 80 (2005) 1244–1251.
[147] A.G. Gayubo, B. Valle, A.T. Aguayo, M. Olazar, J. Bilbao, Energy Fuels 23 (2009) 4129–4136.
[148] X. Guo, Y. Zheng, B. Zhang, Chen, Biomass Bioeng. 33 (2009) 1469–1473.
[149] L. Hong-yu, Y. Yong-jie, R. Zheng-wei, J. Fuel Chem. Technol. 36 (2008) 666–671.
[150] R.K. Sharma, N.N. Bakshi, Bioresour. Technol. 35 (1991) 57–66.
[151] R.V. Pindoria, A. Megaritis, A.A. Herod, R. Kandiyoti, Fuel 77 (1998) 1715–1726.
[152] B. Valle, A.G. Gayubo, A.T. Aguayo, M. Olazar, J. Bilbao, Energy Fuels 24 (2010) 2060–2070.
[159] B. Valle, A.G. Gayubo, A. Atutxa, A. Alonso, J. Bilbao, Int. J. Chem. React. Eng. 5 (2007).
[154] X.X. Zhu, R.G. Mallinson, D.E. Resasco, Appl. Catal. A: Gen. 379 (2010) 172–181.
[155] M. Guisnet, P. Magnoux, Appl. Catal. A: Gen. 212 (2001) 83–96.
[156] A. Ausavasukhi, T. Sooknoi, D.E. Resasco, J. Catal. 268 (2009) 68–78.
[157] M.A. Peralta, T. Sooknoi, T. Danuthai, D.E. Resasco, J. Mol. Catal. 312 (2009) 78–86.
[158] Y. Sendoda, Y. Ono, Zeolites 8 (1988) 101–105.
[159] C.S. Triantafilidis, A.G. Vlessidis, L. Nalbandian, N.P. Evmiridis, Microporous Mesoporous Mater. 47 (2001) 369–388.
[160] Y. Wang, Y. Fang, T. He, H. Hu, J. Wu, Catal. Commun. 12 (2011) 1201–1205.
[161] T. Masuda, Y. Fujikata, S.R. Mukai, K. Hashimoto, Appl. Catal. A: Gen. 172 (1998) 73–83.
[162] W.-C. Cheng, E.T. Habib, K. Rajagopalan, T.G. Roberie, R.F. Wormsbecher, M.S. Ziebarth, in: Handbook of Hetrogenoues Catalysis, Wiley-VCH, 2008, pp. 2741–2777 (chapter 13.2).
[163] EN 590: automotive fuels – diesel – requirements and test methods, 2004.
[164] D.A. Bulushev, J.R.H. Ross, Catal. Today 171 (2011) 1–13.
[165] G. Fogassy, N. Thegarid, G. Toussaint, A.C. van Veen, Y. Schuurman, C. Mirodatos, Appl. Catal. B: Environ. 96 (2010) 476–485.
[166] A.V. Bridgwater, J. Piskorz, in: Progress in Thermochemical Biomass Conversion, Blackwell Wissenschafts-Verlag, 2001, pp. 977–997.
[167] S.B. Jones, C. Valkenburg, C.W. Walton, D.C. Elliott, J.E. Holladay, D.J. Stevens, C. Kinchin, S. Czernik, in: Production of Gasoline and Diesel from Biomass via Fast Pyrolysis, Hydrotreating and Hydrocracking: A Design Case, U.S. Department of Energy, 2009, PNNL-18284.
[168] S. Czernik, R.J. French, C. Feik, E. Chornet, Ind. Eng. Chem. Res. 41 (2002) 4209–4215.
[169] E.C. Vagia, A.A. Lemonidou, Int. J. Hydrogen Energy 32 (2007) 212–223.
[170] D. Wang, S. Czernik, E. Chornet, Energy Fuels 12 (1998) 19–24.
[171] D. Wang, S. Czernik, D. Montané, M.K. Mann, E. Chornet, Ind. Eng. Chem. Res. 36 (1997) 1507–1518.
[172] R. Agrawal, N.R. Singh, AIChE J. 55 (2009) 1898–1905.
[173] N.R. Singh, W.N. Delgass, F.H. Ribeiro, P.K. Agrawal, Environ. Sci. Technol. 44 (2010) 5298–5305.
[174] D. Sanfilippo, P.N. Rylander, in: Ullmann's Encyclopedia of Industrial Chemistry, Wiley, 2009.
[175] F.S. Mederos, J. Ancheyta, J. Chen, Appl. Catal. A: Gen. 355 (2009) 1–19.
[176] H.S. Fogler, in: Elements of Chemical Reaction Engineering, Prentice Hall, 2006.
[177] A. Gianetto, V. Specchia, Chem. Eng. Sci. 47 (1992) 3197–3213.
[178] M.M. Ahmad, M. Fitrir, R. Nordin, M. Tazli Azizan, Am. J. Appl. Sci. 7 (2010) 746–755.
[179] U.S. Energy Information Administration Independent Statistics, 2011, http://www.eia.doe.gov/oog/info/gdu/gasdiesel.asp.
[180] P.A. Horne, P.T. Williams, J. Anal. Appl. Pyrolysis 34 (1995) 65–85.
[181] S.A. Channiwala, P.P. Parikh, Fuel 81 (2002) 1051–1063.
[182] T.J. Thibodeau, A.S. Canney, W.J. DeSisto, M.C. Wheeler, F.G. Amar, B.G. Frederick, Appl. Catal. A: Gen. 388 (2010) 86–95.
[183] J. Wildschut, M. Iqbal, F.H. Mahfud, I.M. Cabrera, R.H. Venderbosch, H.J. Heeres, Energy Environ. Sci. 3 (2010) 962–970.
[184] J. Wildschut, I. Melián-Cabrera, H.J. Heeres, Appl. Catal. B: Environ. 99 (2010) 298–306.
[185] M.V. Bykova, O.A. Bulavchenko, D.Y. Ermakov, M.Y. Lebedev, V.A. Yakovlev, V.N. Parmon, Biocatalysis 3 (2011) 15–22.
[186] V.A. Yakovlev, S.A. Khromova, D.Y. Ermakov, M.Y. Lebedev, V.A. Kirillov, V.N. Parmon, 'Ru2335340c1', Catalyst, method of its preparation (versions) and process of hydrodeoxygenation of oxygen-organic products of biomass fast pyrolysis, 2007.
[187] K. Aasberg-Petersen, T.S. Christensen, I. Dybkjær, J. Sehested, M. Østberg, R.M. Coertzen, M.J. Keyser, A.P. Steynberg, in: Fischer–Tropsch Technology, Elsevier, 2004, pp. 258–405 (chapter 4).
[188] J.R. Rostrup-Nielsen, J. Catal. 85 (1984) 31–43.
[189] J.R. Rostrup-Nielsen, in: Handbook of Heterogeneous Catalysis, Wiley-VCH, 2008, pp. 2882–2905 (chapter 13.11).
[190] M. Sau, C. Narasimhan, R. Verma, Hydrotreatment and Hydrocracking of Oil Fractions, Proceedings of the 1st International Symposium/6th European Workshop, Elsevier, 1997.
[191] G. Valavarasu, M. Bhaskar, K.S. Balaraman, Pet. Sci. Technol. 21 (2003) 1185–1205.
[192] E. Brunner, H. Ernst, D. Freude, T. Fröhlich, M. Hunger, H. Pfeifer, J. Catal. 127 (1991) 34–41.
[193] B. Dawson, M. Spannagle, in: The Complete Guide to Climate Change, Routledge, 2009.
[194] S.P.R. Katikaneni, J.D. Adjaye, N.N. Bakhshi, Energy Fuels 9 (1995) 1065–1078.
[195] A. Oasmaa, D. Meier, J. Anal. Appl. Pyrolysis 73 (2005) 323–334.
[196] Oil-Price.Net, 2011, http://www.oil-price.net/.
[197] P.L. Spath, D.C. Dayton, Preliminary screening—technical and economic assessment of synthesis gas to fuels and chemicals with emphasis on the potential for biomass-derived syngas, Technical report, National Renewable Energy Lab., Golden, CO, USA, 2003, www.osti.gov/bridge.